Sample Return Missions: Rosetta Stones Returned from the First Small Bodies in the Solar System

Tomoki Nakamura, Cecile Engrand, Michael Zolensky, Victoria E Hamilton, Abigail A Fraeman

Sample return missions:

Rosetta stones returned from the first small bodies in the Solar System

Tomoki Nakamura[1*], Cecile Engrand[2], Michael Zolensky[3], Victoria E. Hamilton[4], and Abigail A. Fraeman[5]

[1]Department of Earth Science, Graduate School of Science, Tohoku University Aoba, Sendai, Miyagi 980-8578, Japan, (e-mail: tomoki.nakamura.a8@tohoku.ac.jp)

[2]IJCLab, University Paris-Saclay-CNRS, 91405 Orsay Cedex, France

[3]Astromaterials Research and Exploration Science, NASA Johnson Space Center, Houston, TX 77058, USA

[4]Solar System Science and Exploration Division, Southwest Research Institute, Boulder, CO 80302, USA

[5]Jet Propulsion Laboratory, California Institute of Technology, Pasadena, CA 91109, USA

*Corresponding author: tomoki.nakamura.a8@tohoku.ac.jp

Submitted to Space Science Review on Sep 2nd, 2024

Abstract

It is now possible to bring back samples from planetary bodies of the Solar System other than the moon. This research method enables a direct link between astronomical observations and meteorite analyses, which were previously disconnected. The Hayabusa, Hayabusa2, and OSIRIS REx sample return missions have provided detailed information on the composition of S- and C-type asteroids and the processes by which they were formed. This paper describes (reviews?) the results of these three asteroid sample return missions, and also introduces the next Martian moon sample return mission MMX. Although sample returns are currently achieved only from near-Earth objects in the Solar System, it is hoped that in the future it will be possible to collect samples from outer Solar System objects and even from small objects flying from outside the Solar System.

Competing Interests: The authors declare that they have no conflict of interest.

Introduction

Asteroids and comets are survivors of the first small bodies (planetesimals) formed in the protoplanetary disk about 4.6 billion years ago. Diverse small solid particles were present in the disk. Asteroids and comets retain the characteristics of these solid particles in the disk region where they formed. Therefore, meteorites from asteroids and interplanetary dust from comets reveal details of the chemical evolution of the protoplanetary disk and formation and evolution of small bodies in the early Solar System.

In order to understand the distribution of elements and materials in the protoplanetary disk, it is necessary to determine the distribution of asteroids and comets and their respective elemental compositions and constituent materials. In this respect, the most important point is how accurately we can estimate the constituent materials of asteroids and comets from their reflectance spectra. Comparison of the spectra of meteorites and asteroids has led to investigation of the relationship between the meteorite's chemical type and the asteroid's spectral type (e. g., Britt et al. 1992; Demeo et al. 2022).

However, before the asteroid sample return missions, it was not possible to identify the specific type of asteroids from which the meteorite derived except in a few exceptional cases, such as eucrites from V-type asteroid that is rich in pyroxene and CM carbonaceous chondrites from Cgh and Ch asteroids with 0.7 micron absorption, although the latter relationship needs further confirmation (e. g., Vilas 1989). In order to confirm the asteroid-meteorite relationship with confidence, it was necessary to perform sample returns from asteroids for which spectra had been characterized.

One may think that the composition of asteroids can be estimated by comparing the reflectance spectra of asteroids and meteorites, as mentioned above, without conducting sample return missions. However, there are three problems to be overcome in estimating the composition of asteroids based solely on their reflectance spectra: 1. the spectra of many asteroids are limited to the visible wavelength range, and thus the composition of asteroids, carbonaceous asteroids in particular, is difficult to identify because of a limited number of absorption lines (Bus and Binzel, 2002a, b; Demeo et al. 2009). 2. The spectra of asteroids are affected by space weathering (e.g., Lantz et al. 2017), and the spectra of meteorites are affected by terrestrial weathering (e.g., Amano et al. 2023). These two processes make significant changes in meteorite and asteroid spectra. 3. Spectral properties in the visible to near-infrared are strongly affected by physical properties such as grain size and porosity (e. g., Cloutis et al. 2018), which make both asteroid and meteorite spectral slopes different.

A sample return mission is the only way to directly compare the spectrum of an asteroid taken from a spacecraft with the analysis results of samples recovered from the asteroid. From this comparison, we can know the "correct" answer as to what kind of molecular structures and mineralogical properties are actually responsible for the various absorptions and features, respectively, in the asteroid's spectra. In this way, sample return missions provide important insights into the above three issues that cannot be obtained by any other methods. Therefore, sample return missions have a critical impact not only on the field of meteorite science but also on the field of astronomical observations.

The importance of sample returns extends beyond confirming asteroid-meteorite relationships and deserves a more comprehensive exploration, particularly regarding the preservation of geological context and avoidance of terrestrial contamination. Unlike

meteorites, which lose their original geological setting and are subject to rapid contamination on Earth, returned samples retain their pristine state. This is especially critical for organic-rich materials. Organic compounds in meteorites are highly vulnerable to degradation and contamination from terrestrial exposure, which can obscure interpretations of their origin and pre-solar chemistry. However, by returning material directly from asteroids like Bennu and Ryugu, sample return missions provide access to unaltered extraterrestrial samples within their native geological context. This enables a more accurate understanding of the distribution and nature of organic molecules, crucial for studying early organic chemistry and prebiotic processes in the Solar System.

Four sample return missions from small bodies in the Solar System have been conducted in Japan and the United States of America (Table 1). There have been three asteroid missions and one comet mission. In addition, two sample return missions are planned. Japan Aerospace Exploration Agency (JAXA) developed the Martian Moon eXploration (MMX) mission to take samples from one of the two Martian moons, Phobos, whose origin and formation process are unknown so far (Kuramoto et al. 2021). China National Space Administration plans a sample return mission to a near Earth S-type asteroid (469219) Kamo‘oalewa. The spacecraft Tianwen-2 will launch in 2025 and return to the Earth 2.5 years later. Kamo‘oalewa is a small asteroid (69.45 m × 58.49 m × 51.78 m) with grain size < 2 cm regolith, and rapidly-rotating (period is 27.37 minutes) (Zhang et al. 2024). The visible to near-infrared reflectance spectrum shows a 0.984 μm absorption, similar to LL chondrites (Zhang et al. 2024). Table 1 summarizes the characteristics of the target objects and the outline of each mission except the Chinese Tianwen-2 mission . Figure 1 shows images of all targeted objects at approximately the same scale. Figure 2A shows the visible to near-infrared reflectance spectra of all target bodies.

Table 1. Summary of sample return missions from small sorlar system bodies

Mission	Stardust	Hayabusa	Hayabusa2	OSIRIS-REx	MMX
Type of small body	Short-period comet	S-type asteroid	C-type asteroid	B-type asteroid	Martian moon (D-type asteroid?)
Name	81P/Wild2	Itokawa	Ryugu	Bennu	Phobos
Size (km)	3.3×4.0×5.5	0.54×0.29×0.21	1.04×1.02×0.88	0.56×0.54×0.50	25.90×22.60×18.32
Density (g/cm^3)	0.6-0.8	1.9	1.19	1.19	1.86
Rotation period (h)	-	12.1	7.6	4.3	7.6
Orbital period (days)	2340	557	475	437	7.6 hours around Mars
Semi-major axis (au)	3.45	1.32	1.19	1.13	1.52
Reflectance at 2μm wavelength (%)	-	17	2	2	5
Launch date (yyyy/mm/dd)	1999/2/7	2003/5/9	2014/12/3	2016/9/8	2026 summer (TBD)
Arrival (yyyy/mm/dd)	2004/1/2	2005/9/12	2018/6/27	2018/12/3	2027 Augsut (TBD)
Length of stay around the target (month)	Flyby	3	18	30	40 (TBD)
Earth return date (yyyy/mm/dd)	2006/1/15	2010/6/13	2020/12/5	2023/9/24	2031 winter (TBD)
First sample collection (yyyy/mm/dd)	2004/1/2	2005/11/20	2019/2/21	2020/10/20	not yet determined
Second sample collection(yyyy/mm/dd)	-	2005/11/25	2019/7/11	-	not yet determined
Quantity of recovered sample	many small particles	many small particles	5.4 g	121.6 g	
Major constituent minerals	Olivine Pyroxene Sulfide	Olivine Pyroxene Plagioclase	Phyllosilicates Carbonates Magnetite	Phyllosilicates Carbonates Magnetite	
Sampling methods	aerogel capture	projectile shoot	projectile shoot	gas blow	core burial gas blow
Extended mission target objects	9P/Tempel1	-	Asteroid 2001 CC21 Asteroid 1998 KY26	Apophis (Asteroid 99942)	TBD
References	[1],[2],[3],[4],[5],[6]	[3],[7],[8],[9]	[3],[10],[11],[12],[13],[14]	[3],[15],[16],[17],[18], [19],[20],[21],[22]	[23],[24],[25],[26],[27]

[1] Duxbury et al 2004 [2] Davidsson and Gutiérrez 2006 [3] https://ssd.jpl.nasa.gov/tools/sbdb_lookup.html#/?sstr=81P&view=OPDCA [4] Brownlee et al 2003 [5] Veverka et al 2013 [6] Brownlee et al 2004 [7] Fujiwara et al 2006 [8] Yoshikawa et al 2021 [9] Abe et al 2006 [10] Watanabe et al 2017 [11] Tsuda et al 2020 [12] Kikuchi et al 2020 [13] Hirabayashi et al 2021 [14] Kitazato et al 2019 [15] Lauretta et al 2019 [16] DellaGiustina et al 2023 [17] Simon et al 2020 [18] Barry 2024 [19] Lauretta et al 2015 [20] Williams et al 2018 [21] Wibben et al 2024 [22] Hamilton et al 2024 [23] Carolyn et al 2023 [24] Allen and Cox 2000 [25] Fraeman et al 2012 [26] Kuramoto et al 2022 [27] Nakamura et al 2021

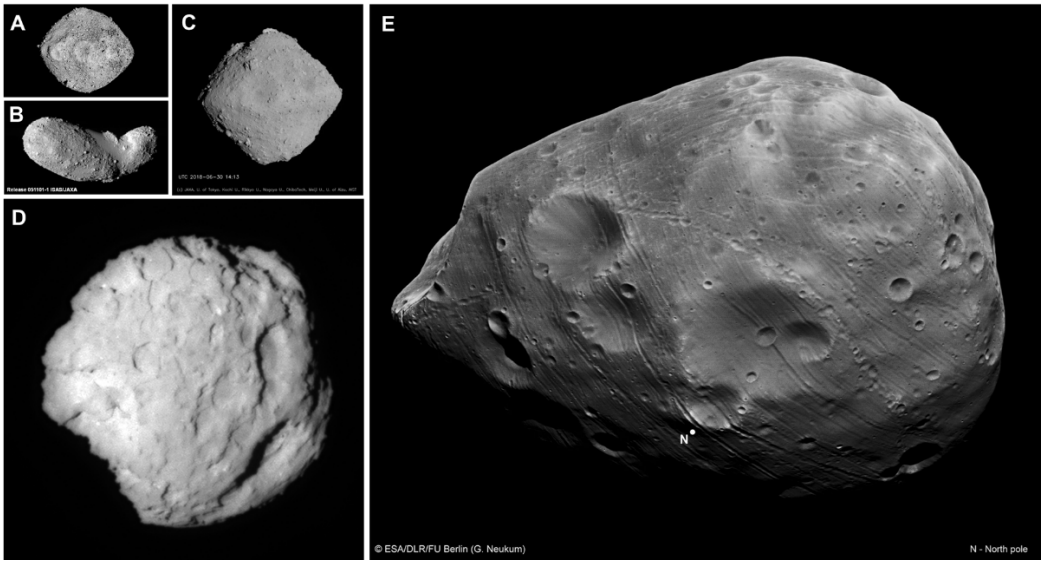

Fig, 1, Targets of the past and future sample return missions in a scale roughly proportional to real size (. (A) Bennu, (B) Itokawa (C) Ryugu (D) 81P/Wild2, and (E) Phobos (maximum dimension of ~27 km). Images from Bennu (https://www.nasa.gov/news-release/nasa-spacecraft-provides-insight-into-asteroid-bennus-future-orbit/), Wild 2 (https://solarsystem.nasa.gov/stardust/photo/cometwild2.html), Itokawa (JAXA digital archives P-043-12077), Ryugu (JAXA digital archives P100011856), and Phobos from North pole (https://mars.nasa.gov/resources/6148/crater-chain-on-phobos/).

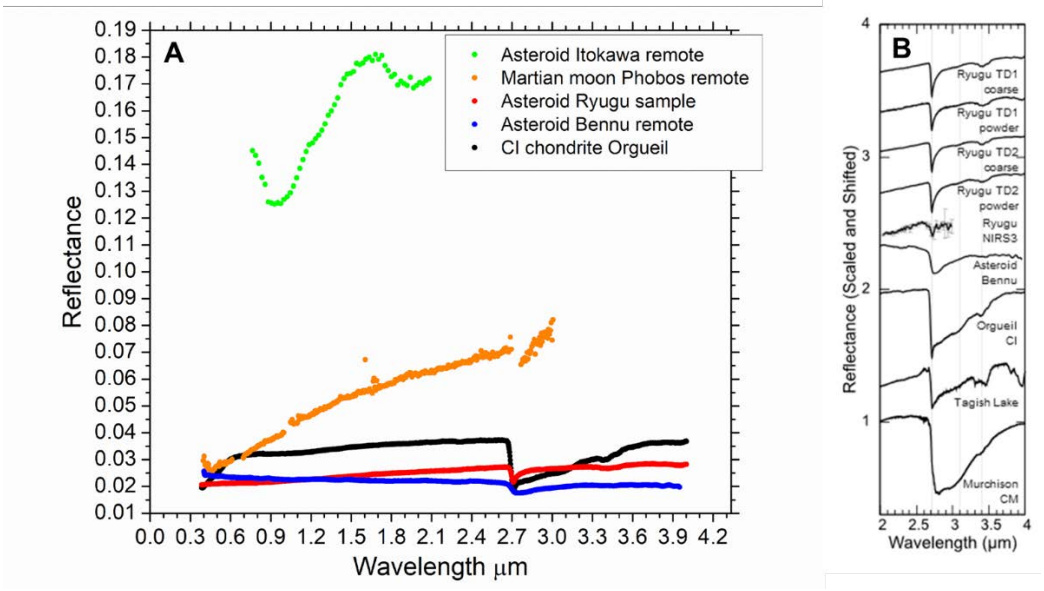

Fig. 2. (A) Reflectance spectra of Solar System small bodies for sample return missions and a CI chondrite meteorite spectrum for comparison. Data of Itokawa from Abe et al. (2006), Phobos from Fraeman et al. (2012), Ryugu and CI chondrite from Nakamura T. et al. (2022), and Bennu from Simon et al. (2020). (B) Variation of 2.7-μm absorption among Ryugu samples, Ryugu remote sensing, Bennu remote sensing, and carbonaceous chondrite meteorites. Data from Nakamura T. et. al. (2022).

The target objects of all missions are near-Earth asteroids and short-period comets that have visited near-Earth orbit. The spacecraft did not recover samples from Main Belt asteroids or the Kuiper Belt. While one-way missions have reached distant Kuiper Belt objects (New Horizons mission: Guo and Farquhar 2008), sample return missions that obviously require a round trip between the Earth and the target object have only brought back samples from objects inside the orbit of Mars. If the sample return mission to the Mars satellite Phobos (Figure 1) by the MMX mission planned by Japan (Table 1) (Kuramoto et al. 2021) and that to Mars planned by the United States of America (Muirhead et al. 2020) succeed, they will break the previous round-trip distance record.

This paper describes the scientific results obtained from the now completed asteroid sample return missions Hayabusa, Hayabusa2, and OSIRIS REx (hereafter O-REx), focusing on remote sensing results. Finally, the MMX mission will be briefly introduced. The sample return mission from the short-period comet 81P/Wild2 is

described in detail in another paper (Zolensky et al. 2024) published in this same special issue.

Hayabusa mission

The Hayabusa mission (Table 1: Kawaguchi et al. 2008) was primarily an engineering mission started in 1995 with the aim of making a round-trip between Earth and a small near-Earth object (the target body was not specified at the beginning) in the Solar System. An S-type asteroid was subsequently selected as the target object because S-type asteroids are abundant in the asteroid belt and considered to be the parent bodies of the most Earth-bound ordinary chondrites, due to the similarity of the reflectance spectra of the meteorites and the asteroids (e. g., Binzel et al. 1996). However, this relationship had not been confirmed at that time.

S-type asteroid 25143 Itokawa (hereafter referred to as Itokawa), which was selected as the mission target in 2000, is a small near-Earth asteroid with a maximum dimension of about 500 m. Itokawa was named after Dr. Hideo Itokawa, the first Japanese rocket developer. Ground-based radar observations of Itokawa in 2001 on its approach to the Earth revealed a rugby ball shape and 12-hour rotation period (Ostro et al. 2004). The so-called YORP effect, a radiation recoil torque affecting the rotation state of small asteroids (Rubincam, 2000), is expected to halve Itokawa's rotation period in 50-90 thousand years (Scheeres et al. 2007).

Hayabusa was launched in 2003, followed by acceleration by an Earth flyby, and arrived at Itokawa in 2005 (Table 1). Hayabusa was the first spacecraft to make an interplanetary flight using ion engines (Kuninaka et al. 2007). Itokawa's surface topography and reflectance spectra were observed from a home position at an altitude of 7 km and a proximity observation at an altitude of 3 to 4 km (e. g., Kawaguchi et al. 2008). Macroscopically, Itokawa has an elongated shape, with a neck at about one-third of its long axis, and a small head and thick body that resemble a sea-otter (Fig. 1B). The size is 535 x 294 x 209 m (Demura et al. 2006), and the density of the object is 1.95 ± 0.14 g/cm^3 (Abe S. et al. 2006), which means that about 40% of the total volume in the object is void space when compared to the density of ordinary chondrite meteorites (Fujiwara et al. 2006).

Eighty percent of the surface of Itokawa is covered by large and small boulders (Saito et al. 2006). The shapes and structures of the boulders are similar to those of rock fragments produced by impact experiments (Nakamura A. et al. 2008). This suggests that Itokawa is a rubble-pile asteroid formed by the reaccumulation of fragments of the original larger body that had been destroyed by a catastrophic impact (Fujiwara et al. 2006), and precise simulations of the impact destruction and reaccumulation of Itokawa's parent body have been performed using N-body numerical codes (Michel and Richardson, 2023).

The age of the catastrophic giant impact has not been determined. Analyses of the recovered samples have provided both relatively young ages (1.3 ± 0.3 Ga by $^{39}Ar/^{40}Ar$ age (Park et al. 2015) and 1.51 ± 0.85 Ga by U-Pb age (Terada et al. 2018)) and relatively old ages (> 2.3 Ga billion years by $^{39}Ar/^{40}Ar$ age (Jourdan et al. 2017) and > 4.2 Ga by $^{39}Ar/^{40}Ar$ age (Jourdan et al. 2023)). It has been suggested that the reason for such long lifetimes for Itokawa-sized small asteroids is due to the shock-absorbing nature of the rubble pile bodies (Jourdan et al 2023).

Detailed analysis of 3D images reveals that Itokawa's surface has undergone extensive landslides, due probably to impact-generated vibration, resulting in the fluidization of the regolith and the formation of the Muses Sea region (Figure 3A), a smooth terrain extending around the body's center of gravity (Miyamoto et al. 2007). The Muses Sea region is composed of millimeter- to centimeter-sized pebbles (Figure 3B: Yano et al. 2006), indicating that size sorting of the constituent particles occurred during fluidization. This means that the surface of an asteroid with low gravity is much more actively modified by the fluidization than previously expected. When the spacecraft approached the surface to collect samples, close-up imaging of the surface was performed at a resolution of up to 6 mm/px. Many of the boulders were found to be aggregates of rock fragments of varying strength or composition (thus breccias), each about 10 cm in diameter, and detailed comparisons have been made with the surface of larger meteorites (Noguchi et al. 2010).

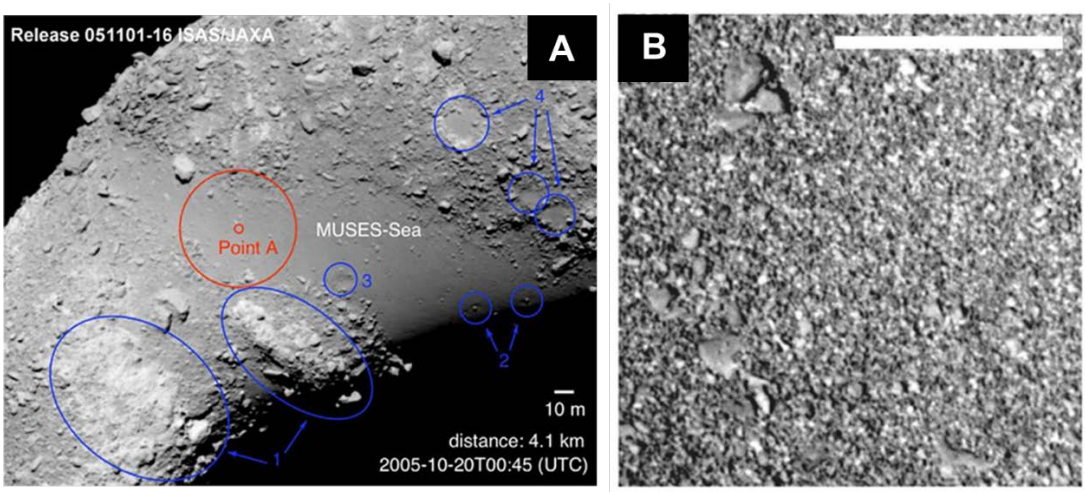

Fig. 3. (A) A whole view of smooth terrain Muses sea area. Touch down site 1 (TD1) is shown as “Point A”. Overall, the Muses sea area has a dark surface, while some areas enclosed by blue circles 1 and 4 are bright areas. (B) Close-up image of TD1 area in Muses sea taken from 63m altitude. The Muses Sea is composed of relatively homogeneous, size-sorted small pebbles ranging from several centimeters to sub-centimeter scales. Scale bar is 1m. Images from Yano et al. (2006).

Visible camera observations from the spacecraft identified bright and dark regions on Itokawa's surface. The dark regions were slightly redder than the bright regions, and the slope of the reflectance spectra was steeper (Saito et al. 2006). The dark regions were distributed over the entire surface of the asteroid, while the bright areas were mostly distributed on inclined slopes and inside craters. This is thought to be due to the fact that vibrations caused by meteorite impacts induced landslides and craters to move and excavated surface materials, exposing bright regions in the deeper layers (Saito et al. 2006). Reflectance spectra in the near-infrared wavelength region show that the spectra of the dark regions have shallower infrared absorption of silicates than those of the bright regions (Abe et al. 2006). From these results, it was inferred that the dark regions are regions that have been altered by space weathering (Saito et al. 2006; Horoi et al. 2006). In particular, the Muses Sea region was a dark region affected by space weathering (Figure 3A). The 1-μm feature of the near-infrared spectra indicated that Itokawa is an olivine- and pyroxene-dominated surface (olivine/(olivine + pyroxene) = 70 ~ 80%), consistent with ordinary chondrite minerals of LL 5-6 (Abe et al. 2006).

Sampling operations were twice performed on the Muses Sea area in November 2005 (Yano et al. 2006: Kawaguchi et al. 2008). The recovery method involved a metal projectile being fired during the final descent of the spacecraft, and the mobilized crushed rock fragments ascended within a sample horn 1 meter tall and were stored in a sample catcher installed inside the spacecraft (Yano et al. 2006). In this process, the spacecraft only touched the surface of the asteroid for a few seconds, so it was defined as a touch-down sample recovery rather than an actual landing. The touch-down operation of the spacecraft was fraught with problems, and sample recovery was extremely difficult. Touch down was successful on both occasions, but no metal projectiles were fired, and it was not known whether the samples were actually recovered until the capsule was opened back on Earth (Kawaguchi et al. 2008).

After the two touch-down operations, the spacecraft experienced many problems and was unable to return to Earth in 2007 as scheduled; instead, it returned to Earth in 2010, three years later than scheduled. A large, state-of-the-art facility to receive samples and perform curation activities was established at ISAS in Japan (Yada et al. 2014). The sample catcher, which was where captured samples should have been, was opened at the Curation Facility without exposing samples to atmosphere (Nakamura et al. 2011), and minute amounts of very small particles (mostly < 0.1 mm) were found inside. Approximately 1500 asteroid particles were identified by separating about 3000 particles from the catcher over a period of about 5 months and analyzing individual particles with an electron microscope (Nakamura et al. 2011). Thus, approximately half of the separated particles proved to be Al metal grains from the walls of the catcher itself. Many more particles have since been identified, and catalogs are available from JAXA curation (https://curation.isas.jaxa.jp/curation/hayabusa/index.html).

Typical Itokawa particles separated from the catcher are shown in Figure 4. Initial analyses were performed using ~50 particles (Nakamura et al. 2011, Yurimoto et al. 2011; Noguchi et al. 2011; Ebihara et al. 2011; Nagao et al. 2011; Tsuchiyama et al. 2011). The results indicate that the Itokawa particles are mainly composed of silicate minerals (olivine, low-Ca pyroxene, high-Ca pyroxene, plagioclase), phosphates (principally merrillite), troilite (FeS), metallic iron (kamacite, taenite), etc. (Nakamura et al. 2011). Water-bearing minerals and organic matter are absent. Recent studies have detected 698 ppm and 988 ppm water in two Itokawa pyroxene grains (Ziliang and Bose, 2019), suggesting that water was somehow supplied to the asteroid before the

formation of pyroxene. Sylvite and halite were also found on the surface of two Itokawa particles (Noguchi et al. 2014). Che and Zega (2023) found nanometer-sized NaCl crystals in association with secondary albitic plagioclase, suggesting a coupled formation process through aqueous fluid activity. This evidence implies that asteroid Itokawa may have experienced hydrothermal processes and challenges the assumption that S-type asteroids, such as Itokawa, were entirely dry compared to C-type asteroids. Instead, they suggest that S-type asteroids may have once supported active hydrothermal systems and could have contributed water to terrestrial planets.

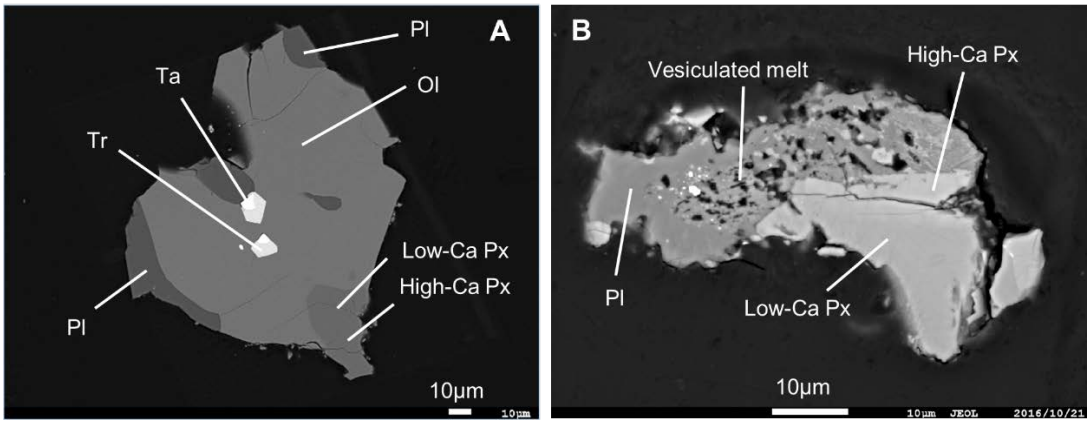

Fig.4. (A) Typical Itokawa particle consisting of well-crystalline olivine, low- and high-Ca pyroxene, plagioclase, and inclusions of taenite and troilite. Silicates compositions are homogeneous and co-existing two pyroxenes indicates equilibrated temperature of 800°C (Nakamura et al. 2011). (B) Itokawa particle consisting of low- and high-Ca pyroxene, plagioclase, and vesiculated melt. The melt was probably formed by an impact. Abbreviation: Ol=olivine, Low-Ca px = low-Ca pyroxene, High-Ca px = high-Ca pyroxene, Pl = plagioclase, Ta = taenite, and Tr = troilite.

The chemical compositions of the silicate minerals are almost homogeneous, which means that Itokawa underwent long-term thermal metamorphism in the interior of the parent asteroid. The average compositional range of olivine is $Fa_{28.6\pm1.1}$, Low-Ca pyroxene is $Fs_{23.1\pm2.2}Wo_{1.8\pm1.7}$, High-Ca pyroxene is $Fs_{8.9\pm1.6}Wo_{43.5\pm4.5}$, and plagioclase is $Ab_{83.9\pm1.3}Or_{5.5\pm1.2}$ (Nakamura et al. 2011). Based on the mean composition and low compositional variability of these silicate minerals, many particles were identified as

being LL5~6 chondrite material. The chemical composition of metallic iron (Nakamura et al. 2011), oxygen isotope ratios (Yurimoto et al. 2011), bulk elemental abundance (Ebihara et al. 2011), and sample bulk density 3.4 g/cm^3 (Tsuchiyama et al. 2011) are also consistent with this interpretation. It was also shown that the constituent minerals and the chemical compositions of the particles recovered from the first and second touchdown sites were nearly identical (Nakamura et al. 2014). This result is consistent with Itokawa's global homogeneous reflectance spectra obtained by the spacecraft (Abe et al. 2006), confirming that asteroid Itokawa is composed almost entirely of LL5~6 chondrite material. Based on the results of remote sensing observations and analyses of the samples returned by the Hayabusa mission, we conclude that the parent bodies of ordinary chondrites are S-type asteroids, as long suspected.

Small asteroids such as Itokawa cannot hold an atmosphere. Therefore, various interactions with materials and radiation in interplanetary space are directly recorded on an asteroid’s surface. One of these is the impact events. The recovered Itokawa samples record shock metamorphism of various intensities (Fig. 4B: also see Zolensky et al. 2022), and the impact stage ranges S2~3 (Stöffler et al. 1991). In addition, interplanetary dust has impacted surface materials and formed micro-craters (Nakamura E. et al. 2012). Matsumoto et al (2018) observed 900 micro-craters (Fig. 5) and concluded that the majority of these were probably formed by secondary-ejecta impacts and the actual crater impact flux seems to be similar between Itokawa and the Moon. The ^{21}Ne cosmic-ray exposure ages of the recovered samples indicate that Itokawa developed its current surface (< ~1 m depth) relatively recently (<8 Ma: Nagao et al. 2011).

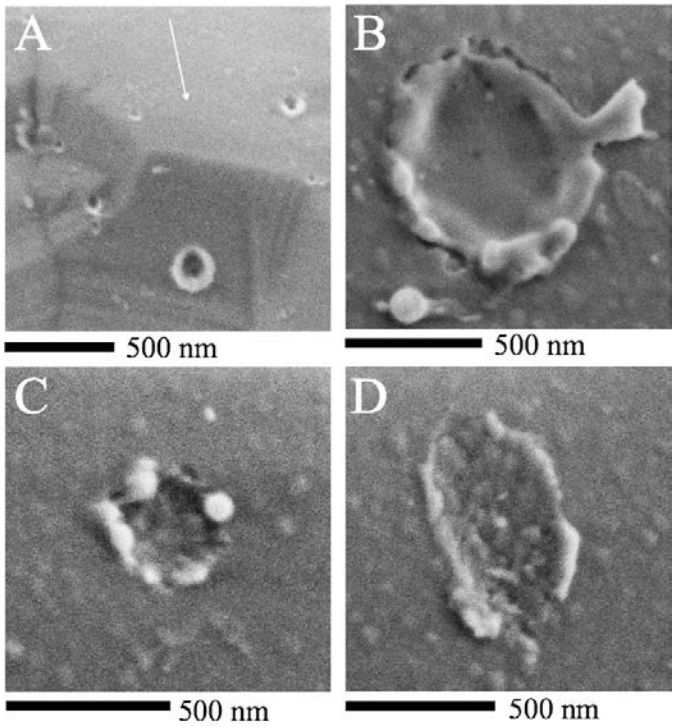

Fig 5: Microcraters found on the surface of Itokawa particles indicating high-velocity impact of interplanetary dust particles (from Matsumoto et al. 2018)

Observations from the spacecraft showed that Muses Sea was reddish-black, and the recovered sample was expected to record space weathering, which was indeed observed (Noguchi et al. 2011). The surfaces of the recovered grains are covered with two altered zones: zone I is an amorphous silicate layer containing nano-phase Fe (npFe). Zone II is mostly crystalline silicate but partially amorphized area. The very surface (5 to 15 nm thick) of zone I is covered with sulfur-bearing Fe-rich nanoparticles (npFe) (Noguchi et al. 2011). The npFe in Zones I and II are thought to have been formed by the reduction of FeO in ferromagnesian silicates by hydrogen supplied by solar wind implantation. On the other hand, sulfur-bearing Fe-rich nanoparticles at zone I may have been formed by the deposition of FeS-containing vapor generated by collision events on the Itokawa surface vaporizing indigenous troilite or other sulfides from the impactors (Noguchi et al. 2011). The formation of tiny opaque particles at the surface of olivine, pyroxene, and plagioclase has been shown to cause darker and redder reflectance spectra of the asteroid.

In addition to zones I and II, vesicular layers were identified in the space weathered

surfaces (Thompson et al. 2014; Noguchi et al. 2014). The vesicles were probably formed by separation of solar-wind derived He implanted in this zone (Noguchi et al. 2014). A pyrrhotite crystal was found to show a disordered rim that is sulfur-depleted and npFe metal grains are decorating the outermost surface (Keller and Berger, 2014). In addition, on the surface of some Itokawa particles, small (~1 μm) metallic iron whiskers are found. It has been proposed that they are a decomposition product formed through irradiation of iron sulfide by energetic ions of the solar wind (Matsumoto et al. 2020).

Based on the chemical composition of low- and high-Ca pyroxene coexisting in Itokawa particles, the thermal metamorphic temperature was estimated to be about 800°C (Nakamura et al. 2011). If the heating source was ^{26}Al, the parent body of Itokawa must have been larger than 20 km in radius and accreted at a period between 1.9 and 2.2 Myr after CAI formation, to satisfy mineralogic and isotopic evidence derived from Itokawa particles (Wakita et al. 2014). In summary, the Itokawa parent body formed in the early Solar System, was heated to a temperature of about 800°C and then cooled slowly. Itokawa was then disrupted by a large impact, and its debris re-accumulated to form the second-generation body called Itokawa. Since then, the surface of the asteroid has been continuously modified by collisions and radiation, and it is only recently that the current surface conditions have been achieved. It remains unclear how and when Itokawa's parent asteroid was disrupted and when Itokawa accreted from some of the remnants.

Hayabusa2 mission

The Hayabusa2 mission (Table 1) aimed to bring to Earth surface samples from the C-type asteroid Ryugu, a near-Earth asteroid (Fig. 1C: Watanabe et al. 2017). Ryugu was classified as Cb-type based on the SMASSII taxonomy and C/F-type following the Tholen taxonomy (e. g., Tatsumi et al. 2020). Pinilla-Alonso et al. (2016) showed that the near-infrared spectrum of Ryugu is similar to the Eulalia and Polana families in the asteroid belt. The collisional lifetime of Ryugu (3-5 × 10^8 yr) is similar to or less than the breakup time of these families 830 ± 150 Myr and 1400 ± 150 Myr for Eulalia and Polana, respectively, and therefore Ryugu might be a member of these families (Sugita et al. 2019).

The spacecraft had almost the same design and functionality as that of the first Hayabusa mission, and the instruments on board were also similar except for the absence of the X-ray fluorescence instrument (Tsuda et al. 2013). The sample recovery method was also the same (Table 1: Sawada et al. 2017). The Hayabusa2 was launched in 2014, made an Earth swing-by in 2015, arrived at the asteroid in 2018, and started observations from an altitude of about 20 km (Tsuda et al. 2020).

Ryugu exhibits a characteristic flattened, spinning top shape (Fig. 1C). Ryugu used to rotate with a shorter period (~3.5h) than today, which is thought to have resulted in a spinning top shape from a spheroidal body (Watanabe et al. 2019). It was suggested that the YORP effect is responsible for the speed up in rotation (Walsh, 2018). The density of the asteroid is 1.2 g/cm^3 (Table 1: Watanabe et al. 2019), which is very low compared to the density of the recovered samples of 1.79 ± 0.08 g/cm^3 (Nakamura T. et al. 2022), indicating that the asteroid interior is more than 30% void space. Thermal inertia ranges from 200 to 500 (av. 300) J.m^{-2}·s$^{-0.5}$·K^{-1} (Okada et al. 2020). This value is much lower than that obtained from the returned samples (< 1 cm in size) (890 J.m^{-2}·s$^{-0.5}$·K^{-1}: Nakamura et al. 2022). This difference is likely due to the presence of large cracks in the surface rocks of the asteroid, which would not be detectable in the < 1 cm sample, and which reduce the heat transfer to the entire body.

Ryugu's surface is composed of many large and small boulders (Fig. 1C and 6A), and there are no smooth terrains such as Itokawa's Muses Sea region. Most of the boulders show similar reflectance spectra, indicating that they formed by the destruction and partial reassembly of a relatively homogeneous original parent asteroid, and therefore Ryugu, like Itokawa, is a rubble pile asteroid (Watanabe et al. 2019). The boulder size distribution and shapes on the entire surface of Ryugu were determined: the shapes of Ryugu's boulders resemble laboratory impact fragments and thus support the interpretation that the boulders were produced by the disruption of Ryugu's parent asteroid (Michikami et al. 2019).

The reflectance of Ryugu is 1.60 ± 0.15 % at 0.55 μm wavelength in standard geometry (Sugita et al. 2019), which is among the lowest in examined Solar System objects (Fig. 2). The visible and near-infrared spectra are very flat, with the only absorption identified at 2.7 microns (Kitazato et al. 2019). The visible and near-infrared spectral slopes (from 0.5 to 0.85 μm wavelengths) do not differ much depending on the location,

but there are red regions with positive slopes (Fig. 6AB: slope > 0.10/μm) and blue regions with near-zero or negative slopes (slope < 0.10/μm), with the blue regions selectively located near the equator and in the polar regions (Sugita et al. 2019). This result indicates that Ryugu's surface was originally made up of blue material, but it has become reddish overall due, probably, to space weathering. The equatorial region, which used to have extended outward more in the past due to then higher rotation velocity, was also a red region. However, as Ryugu's rotation slowed, the red surface near the equator appears to have undergone a landslide and drifted down toward the mid-latitudes, exposing the blue material below the surface (Sugita et al. 2019).

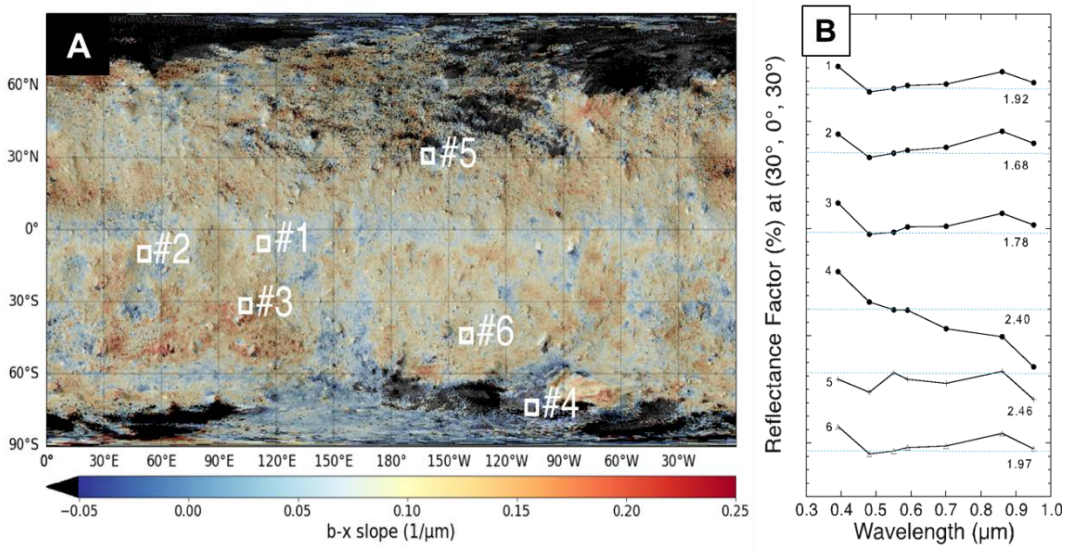

Fig. 6. Multi-band colors of Ryugu surfaces from Sugita et al. 2019. (A) Spectral slope map (μm^{-1}) superposed on a v-band image map, showing redder and bluer regions. The bluer regions locate preferentially equatorial ridge. #1to #6 regions correspond to typical regolith, dark regolith, dark/rugged boulder, Otohime boulder (the largest boulder measures ~130m), bright/mottled boulder, and bright/smooth boulder, respectively. (B) The reflectance spectra of typical morphologic/color features on Ryugu #1 to #6 in panels (A).

The near-infrared spectra of Ryugu are even more uniform than the visible spectra (Fig. 2AB). The 2.7 μm absorption from hydrous minerals was detected globally, indicating that hydrous silicates are present all across Ryugu (Kitazato et al. 2019). Riu et al.

(2021) analyzed NIR spectra of many craters and found that crater floors show a lower reflectance and a deeper 2.7 μm band than their periphery, suggesting that crater floors are more hydrated.

Compared to the spectra of CI and CM hydrous carbonaceous chondrites, Ryugu is darker and has a weaker 2.7 μm absorption feature (Kitazato et al. 2019). Heating experiments of CI and CM chondrites have shown that the reflectance and the 2.7-μm absorption decreases with increasing heating temperature (e.g. Hiroi et al. 1996). Therefore, it was pointed out that Ryugu may be hydrous carbonaceous chondrite material that had been heated to about 500°C and that the hydrous minerals were incompletely dehydrated (Kitazato et al. 2019; Sugita et al. 2019). Other possibilities pointed to hydrated chondritic interplanetary dust particles (IDPs) that experienced lesser aqueous alteration (and were only partially hydrated) of probable asteroidal origin (Kitazato et al. 2019; Sugita et al. 2019; Okada et al. 2020). However, the Ryugu samples recovered on Earth proved to be rich in hydrous silicates with no evidence of heating at high temperatures, nor were they mineralogically similar to chondritic IDPs, hydrated or otherwise (Yokoyama et al. 2022; Nakamura et al. 2022). The reasons for the discrepancy between the interpretation of the reflectance spectrum of asteroid Ryugu and the characteristics of the actual samples are discussed later.

An impact experiment on Ryugu's surface was performed using a small (~ 30 cm in size) impactor with a Cu plate (Arakawa et al. 2020), released from the Hayabusa2 spacecraft between the two sampling efforts. The impact velocity was ~ 2km/s and produced an artificial crater with a diameter >10 m. Subsurface material was ejected from the crater and deposited over a rather wide area due to low gravity (Arakawa et al. 2020). The surface age of Ryugu has been estimated based on the crater size distribution: $(1.58 \pm 0.47) \times 10^8$ years in case for a surface with cohesion or $(8.9 \pm 2.5) \times 10^6$ years for a cohesionless surface (Sugita et al. 2019). The fact that the artificial crater was formed in the gravity-dominated regime on a cohesionless surface supports the latter young age estimation (Arakawa et al. 2020). The young age is also consistent with the cosmic-ray exposure age (on the order of 10^6 years: Okazaki et al. 2023) determined based on cosmogenic noble gas concentrations measured in the returned samples.

It was expected that the vibration induced by the impact experiment would fluidize the

surface of the regolith around the artificial crater and cause resurfacing, but in fact the surface layer was hardly mobilized by the impact. This fact contrasts with the fluid movement of fine-grained material toward the gravity center on Itokawa's surface, which in the case of Ryugu may be due to the rapid attenuation of seismic waves due to the porous nature of the constituent rocks (Nishiyama et al. 2021).

Selection of touch-down sites of the spacecraft was performed using images and spectral data taken at altitudes of 20km, 6km, and 5km (Kikuchi et al. 2020). Hayabusa2 performed multiple low-altitude (~40 m) descending observations, during which spectral and morphological observations were conducted with the highest possible spatial resolutions down to 1 cm/pixel (Fig. 7). The Ryugu surface is well mixed with red and blue areas, but some areas are dominated by blue material and others by red material, depending on the location. The first touchdown sampling site was bluer than the global average (Fig. 7C from Morota et al. 2020). In the region around this first touchdown site, the reddish areas are limited to some boulders, while most boulder surfaces are blue (Fig. 7B and C). These observations are compatible with the interpretation that Ryugu's boulders were originally bluer, with redder materials produced by surface modification processes such as space weathering (Morota et al. 2020).

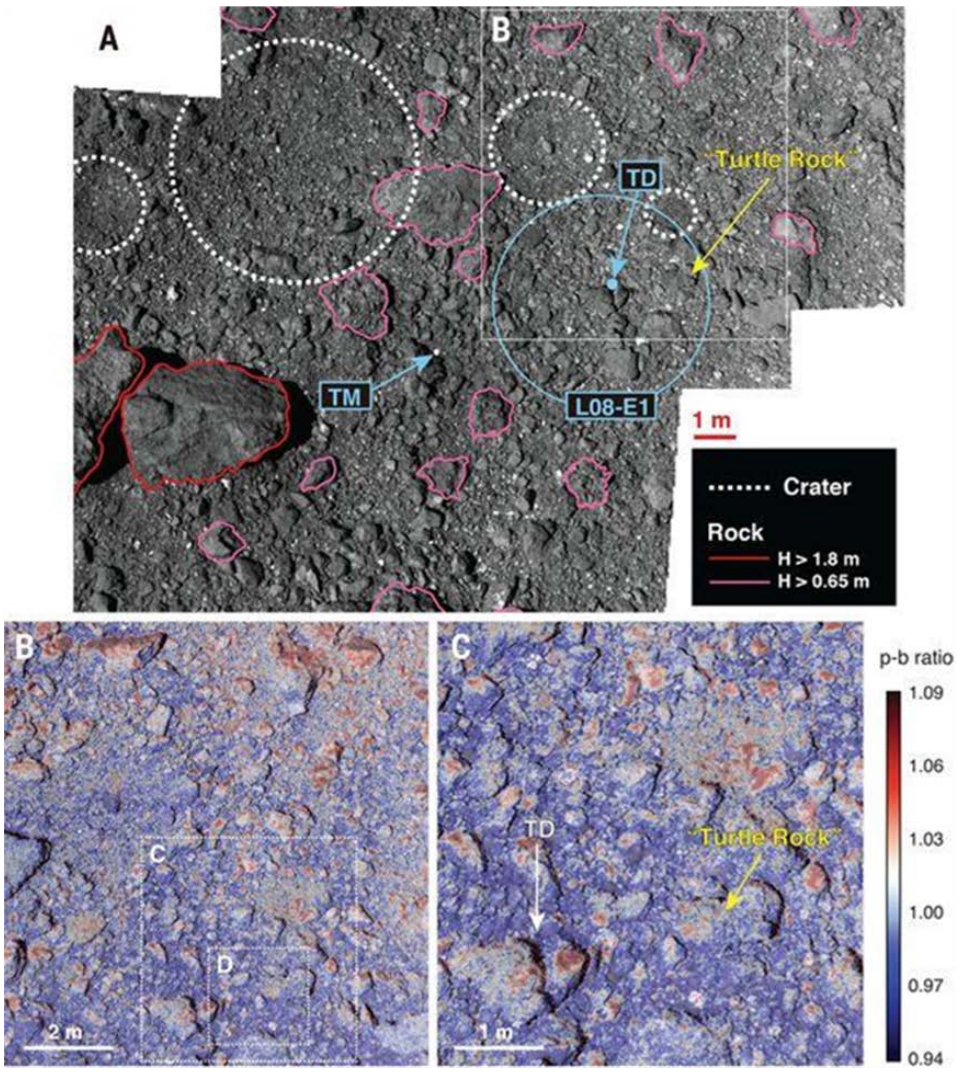

Fig. 7. Morphology and colors around the 1st touch down siteL08-E1 from Morota et al. 2020. (A) Boulder and crater distribution. The light blue arrows indicate the location of the target marker (TM) and the touchdown point of the sampler horn (TD). The light blue circle indicates the L08-E1 area. The white dashed circles indicate craters. Boulder heights (H) were estimated from their shadow lengths; those with H > 1.8 m are outlined in red and those with H > 0.65 m are outlined in pink. The boulder nicknamed Turtle Rock is indicated by the yellow arrow. The white box indicates the region shown in later panels. (B and C) Blue and red area distribution obtained during the touchdown rehearsal operation, from two different altitudes. The dashed box in (B) indicates regions shown in (C).

The second landing site was selected near the artificial crater produced by the impact

experiment, where it was confirmed that material ejected from the crater had accumulated (Tachibana et al. 2023). Unlike the troubled Hayabusa's touchdown operations, in which no bullets were fired due to a series of problems, the sample collection of Hayabusa2 was performed twice without problems, and the camera attached to the base of the sampling horn observed that the surface rocks were crushed with many fragments being scattered by the projectile firing (Tachibana et al. 2023).

The return capsule landed in the Woomera Desert in Australia, as did the Hayabusa mission capsule (Table 1). The day after the capsule returned to Earth, a trace amount of gas was collected from the sample container. The isotopic ratios of helium and neon in the gas indicated that the gas was a mixture of solar wind and Earth's atmosphere (Okazaki et al. 2022). The capsule was then quickly transported to Japan, where the container was opened and the recovered samples were initially examined (sample weighing, spectral analysis, etc.) for about six months at the ISAS curation facility developed specifically for Ryugu samples (Yada et al. 2022). A total of 5.4 g of samples were collected by the Hayabusa2 spacecraft, with the largest individual fragment being about 1 cm in diameter. Most of the collected particles were smaller than a few millimeters in size. Spectral measurements in the visible and near-infrared wavelength regions showed that the samples exhibit 2.7 μm absorption of hydrous silicates (Fig. 2AB), consistent with asteroid spectra obtained from the spacecraft (Yada et al. 2022; Pilorget et al. 2022).

The morphology and polished surface of a large Ryugu sample is shown in Figure 8A. Following the initial description work at ISAS, initial analyses were conducted by eight groups in Japan, and the bulk chemical composition was found to be very primitive, close to solar and CI chondrites (e. g., Yokoyama et al. 2022; Nakamura E. et al. 2022; Ito et al. 2022). Muon beams were applied for the first time to the analysis of samples recovered from asteroids, permitting an elemental composition, including the light elements C, N, O, which matched CI chondrites for most elements. However, oxygen was found to be about 1/3 less abundant than in CI meteorites (Nakamura T. et al. 2022; Ninomiya et al. 2023). Petrographic analysis indicated that the Ryugu sample is similar to CI chondrites, with the samples being dominated by hydrous silicates and carbonates that indicate pervasive aqueous alteration and lacking millimeter-sized chondrules (Fig. 8A and B from Nakamura T. et al. 2022). The samples contain a high concentration of

carbon (4.6 wt%), mostly in the form of insoluble organic matter, and bio-related molecule soluble organic matter such as amino acids (Yabuta et al. 2022; Naraoka et al. 2023). In addition, the samples contain high concentrations of primordial noble gases such as Ar, Kr, and Xe (Okazaki et al. 2023). Concentrations are 1.5×10^{-6}, 2.0×10^{-8}, and 1.9×10^{-8} cm^3 STP g^{-1} for ^{36}Ar, ^{84}Kr, and ^{132}Xe, respectively, and these concentrations are close to the highest value found in a CI chondrite (Okazaki et al. 2023).

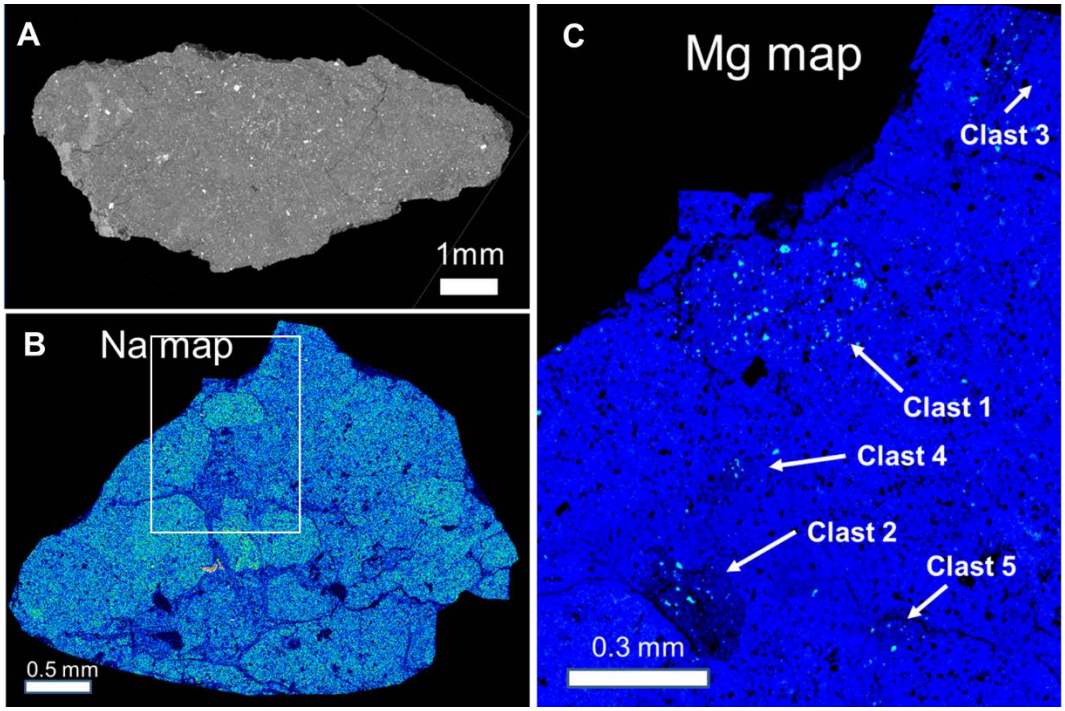

Fig. 8. Internal texture of the largest 2nd touch down sample C0002 from Nakamura T. et al. 2022. (A) CT image of the largest cross section indicating the absence of normal-size (~ 1mm) chondrules and CAIs observed in other chondrites. (B) Na map of the real cross section taken by electron microscope, showing that C0002 is a breccia of many small clasts with variable Na concentrations. (C) Mg map of a portion enclosed by white box in (B). There are many clasts containing bright spots of Mg which are olivine and pyroxene. These clasts are less altered compared with surrounding major lithology.

Spectral observations from the spacecraft revealed a global abundance of hydrated

silicates (Kitazato et al. 2019). The recovered samples were also found to be rich in hydrated silicates, and the almost complete absence of anhydrous silicates indicates that the Ryugu parent body was rich in liquid water at some earlier time, resulting in extensive aqueous alteration over a wide area of the entire asteroid (Yokoyama et al. 2022; Nakamura T. et al. 2022). The hydrous silicates are mainly Mg-rich saponite and serpentine with Mg/(Mg + Fe) ~ 0.8-0.9, and locally small amounts of Mg-chlorite. Carbonate minerals are dominated by dolomite and breunnerite. Phosphorus phase is dominated by apatite, but small amounts of phosphides such as $(Fe, Ni)_3P$ also occur. Iron sulfides are mostly pyrrhotite with some pentlandite (Nakamura T. et al. 2022; Noguchi et al. 2023). Aliphatic organics and phyllosilicates occur together indicating a genetic relationship (Ito et al. 2022; Dionnet et al. 2023; Aléon-Toppani et al. 2024). All of these major constituent minerals were formed by aqueous alteration, and their elemental compositions, isotopic compositions, and crystal structures should record the physico-chemical conditions during the alteration.

Water temperatures during the alteration were estimated from the oxygen isotope ratios of co-existing carbonate minerals and magnetite, which were low between 0 and 20 °C (McCain et al. 2023) at the onset of the alteration, but later increased to between 9 and 20 °C (Nakamura E. et al. 2022) and 37 ± 10°C (Yokoyama et al. 2022). In addition, alteration temperatures have been inferred from mineralogical evidence. Based on the composition of coexisting pentlandite and pyrrhotite, the temperature was estimated to be about 25 °C and, based on the site occupancy of Fe and Ni in the pentlandite crystal structure, it was about 20 °C (Nakamura T. et al. 2022). The change in carbonate mineral type (from Ca carbonate to CaMgFe carbonate) with the progression of alteration is also inferred from the oxygen and carbon isotope ratios of various carbonate minerals (Fujiya et al. 2023). The Ryugu samples preserve rock fragments with different degrees of the alteration, which apparently recorded the multistage geological evolution of the Ryugu parent body (Yamaguchi et al. 2023).

By applying ^{53}Mn-^{53}Cr chronometry to the carbonate minerals, the ages of carbonate formation were estimated to be 1.8 Myr (McCain et al. 2023), 2.6 Myr (Nakamura E. et al. 2023), and 5.2 Myr (Yokoyama et al. 2022) after CAI formation. Although the early value of 1.8 Myr is debated due to potential analytical issues, these results indicate that Ryugu's parent body was formed in the early Solar System, followed by hydrothermal

alteration episode(s) that happened on the parent body a few million years after CAI formation. Thermodynamic equilibrium calculations were performed using the bulk chemical composition of Ryugu samples for the case of the water temperature range of 0, 20 and 40°C, and the coexisting mineral species and mineral abundances were estimated as a function of water rock ratios of the Ryugu parent asteroid (Nakamura T. et al. 2022). By comparing the mineral species and mineral abundances in the actual samples, it was estimated that the highly-altered major lithology that makes up the majority of Ryugu samples was formed by water-rock-weight ratios of 0.2-0.9 (approximately 1 by volume ratio) (Nakamura T. et al. 2022).

Ryugu contains a carbon abundance of 4.63 ± 0.23 wt%, consisting of ~ 65% organic carbon and ~ 35% of the carbon in carbonates. The organic carbon abundance amounts to 3.08 ± 0.3 wt%, which is similar to the values observed in the Ivuna chondrite (Yokoyama et al. 2022). The bulk nitrogen abundance of Ryugu samples is ~ 0.15 wt%, which leads to a N/C atomic ratio of 0.01 to 0.035, a range of value that is comparable to that in primitive carbonaceous chondrites.

The organic signature of Ryugu samples was analyzed both for the soluble organic matter (SOM) and insoluble organic matter (IOM). The characterization of the SOM of Ryugu samples by FT-ICR (Fourier Transform - Ion Cyclotron Resonance) mass spectrometry and by GC×GC - HRMS (multidimensional gas chromatography coupled with high resolution mass spectrometry) showed a very high molecular diversity, and similarities with that of CI chondrites (Naraoka et al. 2023; Schmitt-Kopplin et al. 2023; Aponte et al. 2023). Low temperature and water-rich conditions on the parent asteroid are suggested by the absence of organo-magnesium species and high contents of sulfidic and nitrogen-rich compounds, as well as ammonium ions. PAHs are present in a structural continuum of carbon saturations and oxidations, suggesting several episodes of low temperature aqueous alteration, or a potential origin of these PAHs from the interstellar medium (Naraoka et al. 2023; Schmitt-Kopplin et al. 2023; Aponte et al. 2023; Zeichner et al. 2023). Hashiguchi et al. (2023) found that the spatial distributions in Ryugu samples of CHO, CHN, CHON, CHO-Na molecular ions are not strictly similar, suggesting different timing of precipitation of different transportation mechanisms and/or possible interactions between organics and minerals.

Amino acids were identified in chambers A and C Ryugu samples, with glycine and β-

alanine being detected at the ppm level (Naraoka et al. 2023; Potiszil et al. 2023; Parker et al. 2022, 2023). There is no enantiomeric excess detected in the amino acid distributions, strongly suggesting the absence of terrestrial contamination (Parker et al. 2022, 2023). Aliphatic amines (e.g. C1-C5 chains) were also identified in Ryugu samples, with a decreasing abundance when increasing the chains' length (Naraoka et al. 2022; Parker et al. 2022, 2023). The concentrations and relative distributions of amino acids and aliphatic amines in Ryugu samples are somewhat different from that in Orgueil (Parker et al. 2023). This might be due to different initial compositions, or to different alteration processes on the asteroid or on Earth. The β-alanine/glycine ratio for samples from chamber A and chamber C samples are 0.57 and 1.03, respectively (Potiszil et al. 2023). As this ratio decreases with increasing aqueous alteration, this result suggests that the chamber A sample underwent a larger extent of aqueous alteration than the chamber C sample. Uracil was also found in Ryugu samples by Oba et al. (2023). Uracil being one of the four nucleobases in ribonucleic acid, this highlights the importance of such a molecule for a prebiotic delivery on the early Earth.

As a whole, the SOM components are less abundant than in type 2 chondrites like CM meteorites, and are more similar to that of CI chondrites, which is in agreement with the chemical and mineralogical composition of Ryugu samples being close to that of CI chondrites. Various long duration aqueous alteration processes on the Ryugu parent body are probably needed to explain the different types of SOMs identified in Ryugu samples (e.g. Naraoka et al. 2023). The Mn-Cr dating of carbonate formation ages in Ryugu samples also suggest the possibility of several aqueous alteration episodes, a few million years after CAI formation (see above).

Organic matter was also studied in whole-rock samples by in situ spectro-imaging techniques, and insoluble organic matter (IOM) extracted from Ryugu samples by acid etching was analyzed by the same techniques. The characterization methods included Fourier-transform infrared microscopy (μ-FTIR), infrared nano-spectroscopy (AFM-IR), scanning transmission X-Ray spectroscopy (STXM-XANES), and Raman spectroscopy (Yabuta et al. 2023; Dartois et al. 2023; Kebukawa et al. 2024; Mathurin et al. 2024; Phan et al. 2024; Bonal et al. 2024; Quirico et al. 2024; Ito et al. 2022; De Gregorio et al. 2024).

The μ-FTIR spectra of the Ryugu organic matter shows similarity with that of

carbonaceous chondrites, both in whole-rock and IOM samples (Figure 9, Yabuta et al. 2023; Kebukawa et al. 2024; Dartois et al. 2023; Quirico et al. 2024). The AFM-IR and STXM-XANES analyses that could study the distribution of organic matter at the sub-µm level revealed that the organic matter in whole-rock samples is present in two forms, as a diffuse phase intermixed with the phyllosilicate matrix, and in the form of organic patches, which often resemble nanoglobules found in primitive carbonaceous chondrites (Figure 10). The diffuse phase shows a signature dominated by aromatic C=C, with the presence of carbonyl C=O and aliphatic CHx. The organic patches have a composition which is enriched in C=O and aliphatic CHx compared to the diffuse phase (Figure CE2), which could be explained by a formation of these organic patches (and nanoglobules) by irradiation of ices in the protoplanetary disk (Mathurin et al. 2024).

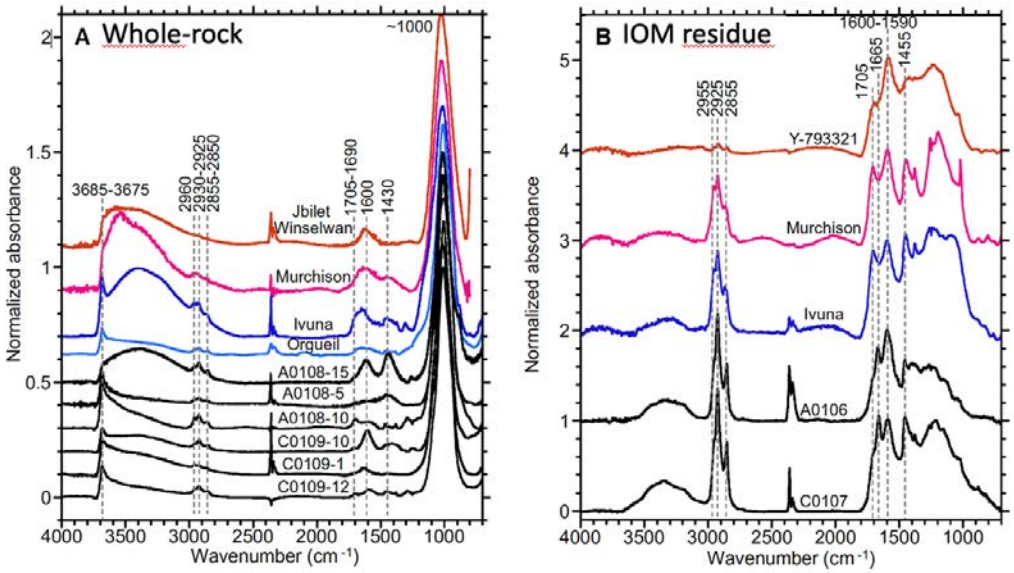

Fig 9: (a) Infrared transmission spectra of six Ryugu intact grains from A0108 and C0109 (black), CM chondrites Jbilet Winselwan (red) and Murchison (pink), and CI chondrites Orgueil (light blue) and Ivuna (dark blue). All the spectra were baseline corrected using spline curves and normalized by the peak height of the band at ~1000 cm^{-1}. (b) Same as (a) but for insoluble organic matter (IOM) residues from Ryugu samples A0106 and C0107 compared with IOM from CM chondrites Y-793321 and Murchison, and CI chondrite Ivuna. The spectra were baseline corrected using spline curves and normalization to the peak height of the aromatic C=C band at ~1600 cm^{-1}. (Adapted from Yabuta et al., 2023).

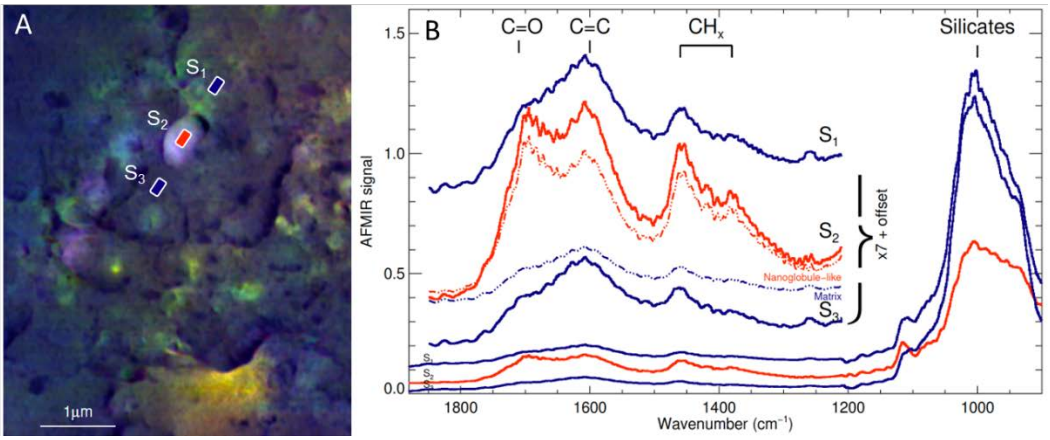

Fig10 : Whole-rock Ryugu sample A0108-19 crushed on a diamond window. (a) Infrared nanospectroscopy (AFM-IR) RGB image of showing the contribution of C=O (red, 1720 cm^{-1}); C=C (green, 1600 cm^{-1}); CH_X (blue, peaked at 1460 cm^{-1}). (b) spectra corresponding to the areas S1 to S3 shown in (a), showing the presence of a diffuse phase (blue spectra), and of a nanoglobule-like feature visible in the S2 location in (a) (red spectra). Adapted from Mathurin et al. (2024).

The composition of IOM extracted from Ryugu samples in chamber A and chamber C show differences in their N content, with average formulas being $C_{100}N_1O_{10}S_{0.8}$ and $C_{100}N_2O_{10}S_{0.8}$, respectively (Yabuta et al. 2023).

Raman and µ-FTIR analyses of Ryugu samples did not show evidence for long duration thermal metamorphism, but variabilities between samples may have recorded low amount of heating possibly due to impacts on the asteroidal parent body (Bonal et al. 2024; Quirico et al. 2024).

An unexpected N-H rich component was identified early in Ryugu samples by reflectance spectroscopy. This phase was first described as a NH_4-rich phase, maybe in the form of ammoniated phyllosilicates, NH_4 hydrated salts, or N-rich organics (Pilorget et al. 2022). Based on an in-depth analysis, Pilorget et al. (2024) then reported the discovery of a unique class of phosphorus-rich grains with major biochemical potential. These grains are up to a few hundreds of µm in size, and have a hydrated-ammonium-magnesium-phosphorus (HAMP)-rich composition. Their compositions suggest an outer Solar System origin. On the prebiotic Earth, an input of such phosphorus and nitrogen-rich phases could have played an important role in the biochemical evolution

of organic matter. Based on X-ray diffraction studies of Ryugu samples, Viennet et al. (2023) suggested that N-rich organics could be trapped in the interlayer space of smectite in Ryugu samples. N-rich outlier phases were also observed by μ-FTIR in IOM samples by Kebukawa et al. (2023) and Quirico et al. (2024). The compositions of these N-rich phases were not well constrained, but Kebukawa et al. (2023) propose a N-H functionality (likely amide) for one of the N-rich phases.

Although being exposed to space at the surface of asteroid Ryugu, organic components, including soluble organic matter, are preserved in Ryugu samples. This demonstrates the robustness of these compounds with regard to space weathering, and the possible delivery of prebiotic molecules from interplanetary materials to the early Earth.

Most of the Ryugu samples are breccias, consisting of small rock fragments ranging from a few tens of microns to a few millimeters in size (Fig. 8B and C). The majority of the rock fragments show highly-altered lithology as described above, while some fragments are less altered (Fig. 8C). The main characteristics of these less-altered fragments are that they contain fine particles (mostly less than 10 μm) of anhydrous silicates such as olivine and low- and high-Ca pyroxene (Fig. 8C) and that their mineral combination is different from that of the altered fragments (Table 2: Nakamura T. et al. 2022). The least altered fragments contain amorphous silicate similar to GEMS, which is not contained in the less altered fragments (Nakamura T. et al. 2022). The mineral assemblages and their relative abundances of the less-altered fragments are similar to those expected under alteration conditions with low water-rock ratios (water-rock weight ratio 0.1-0.2) based on thermodynamic calculations (Nakamura T. et al. 2022). Therefore, the less altered fragments were located in relatively water-poor areas in the Ryugu parent body, and thus retain more information about Ryugu's precursor materials, i.e., information at the time of accretion (Nakamura T. et al. 2022). In fact, a high concentration of presolar grain SiC was found in one Ryugu fragment with a low degree of alteration (Nguyen et al. 2023).

Table 2. Constituent mienrals of the less altered and altered fragments in Ryugu samples (data from Nakamura T. et al. 2022)

	Less-altered fragments	Altered fragments
Anhydrous silicates	small (< 10 micron) olivine, low-Ca and high Ca pyroxene, spinel, and perovskite	none
Hydarated silicates	amorphous silicates (in the least-altered fragments) to poorly crystalline phyllosilicates	saponite and serpentine
Carbonates	minor amounts of Ca carbonate (calcite and aragonite)	dolomite and breunnerite
P phases	minor phosphide $(Fe, Ni)_2P$ or $(Fe, Ni)_3P$ and NaMg phosphate	apatite
FeS phases	submicron pyrrhotite	sumicron pyrrotite and pentlandite and and large hexagonal pyrrhotite

NaMg phosphate is found as small particles (~ a few microns or less) in the least altered clasts and as relatively large veins in the less altered clasts (Fig. 11A). The texture and occurrence indicate that the phosphate formed during an early stage of aqueous alteration. The chemical composition in wt % of the NaMg phosphate is: MgO 26.34, P_2O_5 47.48, Na_2O 1.74, FeO 0.44, Cl 0.20, total 76.2, showing an atomic ratio of Mg/P = ~1, which indicates a possible formula of $Mg_2P_2O_7$-4(H_2O) or $Mg(PO_3OH)$-1~2(H_2O) (Ma et al. 2022). TEM observation revealed that the NaMg-phosphate is amorphous and vesiculated (Fig. 11B: Nakamura et al. 2022). EBSD analysis confirms that the present Mg-phosphate is amorphous (Ma et al. 2022). These results suggest that the NaMg phosphate was originally enriched in volatiles such as water and or organics which later evaporated, resulting in the vesiculated texture. The daytime temperature of Ryugu's surface at its current orbit is ~80°C (Shimaki et al. 2020) and the NaMg phosphate might have been heated and vesiculated at this temperature. NaMg phosphate is also widely found in the Bennu sample and has been found to be similarly amorphous (Barnes et al. 2024). Possible similar amorphous Mg phosphates have recently been reported in the CI chondrite meteorites (Mikouchi et al. 2024).

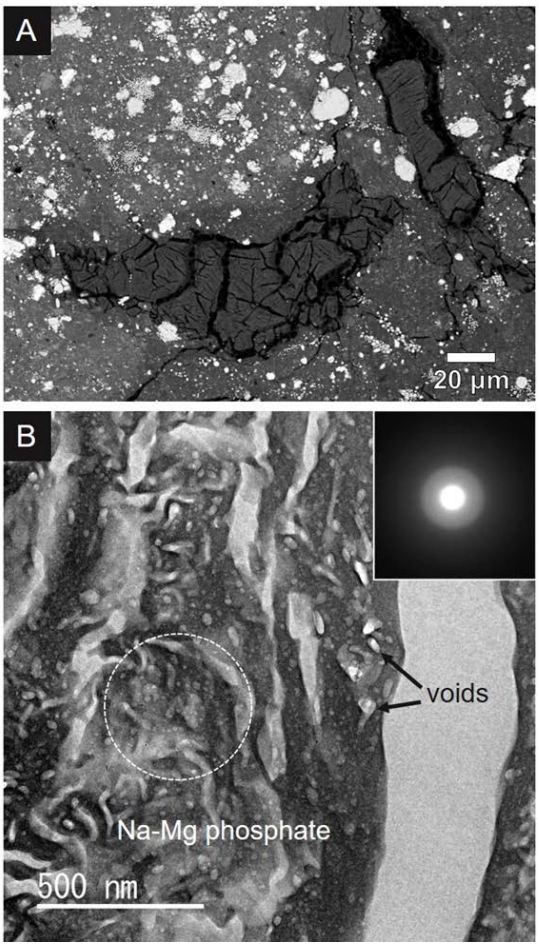

Fig. 11. NaMg phosphate in C0002 from Nakamura T. et al. 2022. (A) Back-scattered electron image of NaMg phosphate with wrinkled texture. (B) Bright field TEM image of the NaMg phosphate. The NaMg phosphate exhibits a vesicular texture suggesting vaporization of volatile molecules. The inset is a selected area electron diffraction pattern obtained from the area indicated by a white circle suggesting that the N-Mg phosphate is an amorphous phase.

High-resolution (< 1 μm) synchrotron radiation CT analysis revealed that chondrules and CAIs of sizes that are abundant in chondrites are not present (Fig. 8A and also see Ito et al. 2022). On the other hand, a small number of very small (< 30 μm) chondrules and CAIs were found in the aforementioned less altered Ryugu fragments (Nakamura T. et al. 2022). The chondrules are type-I POP and BO, and the CAIs are composed of spinel, hibonite, and perovskite. Oxygen isotopic analysis by SIMS showed that all CAIs have a ^{16}O-rich composition, which is the same isotopic composition as that of

CAIs in carbonaceous chondrites (Nakashima et al. 2023). On the other hand, the chondrules showed ^{16}O-rich and ^{16}O-poor compositions, with the ^{16}O-rich compositions similar to AOA and the ^{16}O-poor compositions similar to chondrules (Nakashima et al. 2023). This result is consistent with the presence of the two types (^{16}O-rich and ^{16}O-poor) of small olivine particles scattered in many Ryugu samples (Kawasaki et al. 2022; Liu et al. 2022; Nakamura E. et al. 2022). The formation process of high-temperature objects in Ryugu samples such as CAIs, chondrules, and AOAs, as well as their accretion process to the Ryugu parent body, are not well understood and therefore require further study.

There is much evidence that Ryugu's parent body formed in a low-temperature region in the protoplanetary disk, including the presence of ^{15}N-rich organic matter (Ito et al. 2022), the presence of liquid water containing CO_2 (Nakamura T. et al. 2022), and the abundance of carbonate minerals in the entire recovered samples (Loizeau et al. 2023). Based on the above observations, Ryugu's parent body is considered to have formed at > 10au below -200℃ outside the CO_2 snow line. The fact that Ryugu contains few chondrules and CAIs, and that they are as small as most chondrules and CAIs in comet samples from 81P Wild2 (Zolensky et al. 2006; Nakamura et al. 2008) is also consistent with their formation at the outer edge of the Solar System.

Ryugu samples show Fe isotopic anomalies similar to Ivuna-type CI chondrites, which are distinct from all other carbonaceous chondrites, suggesting that Ryugu and CIs constitute an isotopically distinct third reservoir located at the outermost protoplanetary disk (Hopp et al. 2022). Cu and Zn isotope signatures also indicate that Ryugu and CI belong to the distinct third reservoir (Paquet et al. 2023). This suggests that there has been an isotopic trichotomy between NC, CC, and Ryugu/CI in the Solar System. On the other hand, an interpretation that Ryugu and CI are part of the CC based on the Te-Fe isotopic correlation has been proposed and is under discussion (Marrocchi et al. 2023). Future isotopic analyses of the less-altered fragments will help us to understand whether Ryugu is material from a distinct third reservoir in the protoplanetary disk.

Observations of asteroids from the ground and space have progressed, and asteroids have been classified based on their spectral characteristics (Bus and Binzel, 2002; DeMeo et al. 2009). Comparison of spectra between carbonaceous chondrites and C- and D-type asteroids suggests that these asteroids are made of carbonaceous chondrites

or similar materials. For the first time in the Hayabusa2 mission provided the first opportunity to obtain both the spectra of asteroids and the spectra of samples recovered from the same asteroids, and compare them in detail. The samples from the first Hayabusa mission were too minute for this to be usefully done. As a result, unexpected results were obtained: (1) Visible and near-infrared spectra of the asteroid obtained by the spacecraft (Sugita et al. 2019; Kitazato et al. 2019) and the spectra of the recovered sample are roughly consistent (Pilorget et al. 2022), but the 2.7-μm absorption depth from hydrous minerals is about twice as deep in the samples (Fig. 2B). (2) The spectra of the CI chondrite Orgueil and Ryugu samples, which are nearly identical in mineralogy and petrology, differ significantly (Fig. 2A), with the Ryugu samples being darker, monotonous, and having a less 2.7-μm absorption (Nakamura T. et al. 2022).

Since these two problems have a significant impact on future observations of asteroids and the interpretation of the obtained spectra, they were examined in detail. The conclusion is that the cause of these spectral discrepancies is space weathering of asteroids and terrestrial weathering of meteorites. The main cause of the discrepancy in (1) is space weathering. The topmost surfaces of asteroids are constantly exposed to solar wind and cosmic dust bombardment, causing space weathering and various surface transformations (Noguchi et al. 2023; Matsumoto et al. 2024). Therefore, asteroid spectra obtained from spacecraft are characterized by heating and incomplete dehydration due to space weathering. On the other hand, the recovered samples were crushed by a metal sphere at the time of sample collection, exposing a fresh surface. Therefore, the spectra of recovered samples are dominated by spectra that have not been subjected to space weathering (Matsuoka et al. 2023). This is why the spectra of the recovered samples are different from those of the remote observation.

Meanwhile, the spectral discrepancy in (2) is due to terrestrial weathering: after falling to the Earth, CI chondrites rapidly react with the Earth's oxygen and water, resulting in significant weathering. As a result, Fe^{2+} in the hydrous mineral saponite is oxidized (Roskosz et al. 2023) and becomes brighter (Nakamura T. et al. 2022). In addition, the oxidation of small pyrrhotite crystals forms bright hydrous Fe sulfate, which brightens the overall sample and deepens the absorption at 2.7-3.0-μm (Amano et al. 2023). Thus, the spectra of CI chondrites change as they are weathered on the ground, and their spectra differ significantly from those of CI materials that have not been weathered at

all, such as Ryugu. That terrestrial weathering is the cause of the spectral discrepancy is proved by the fact that when CI chondrites are heated in a reducing environment to a temperature at which hydrous minerals do not decompose (about 300°C), the spectra of the heated CI and the Ryugu sample are almost identical (Amano et al. 2023). The degree of spectral change of CI materials is greater by terrestrial weathering than by space weathering. Thus, the spectra of asteroids composed of these reactive materials should be interpreted with caution when we compare them to corresponding meteorite spectra.

Asteroid Ryugu is the first asteroid for which the physical properties of recovered samples were measured in detail: Density, mechanical properties, and thermal properties were determined (Nakamura et al. 2022; Ishizaki et al. 2023). A thermal evolution model of Ryugu's parent body with ^{26}Al as a heat source was constructed using the specific heat, thermal diffusivity, and water-rock ratio estimated from the mineral abundances of the Ryugu samples (Nakamura T. et al. 2022). A simulation of the collisional destruction of the Ryugu parent body was also performed using the measured sample strength and elastic velocities (Nakamura T. et al. 2022). A model of the formation, evolution, and collisional destruction of the Ryugu parent body was constructed using these sample measurements (Fig. 12).

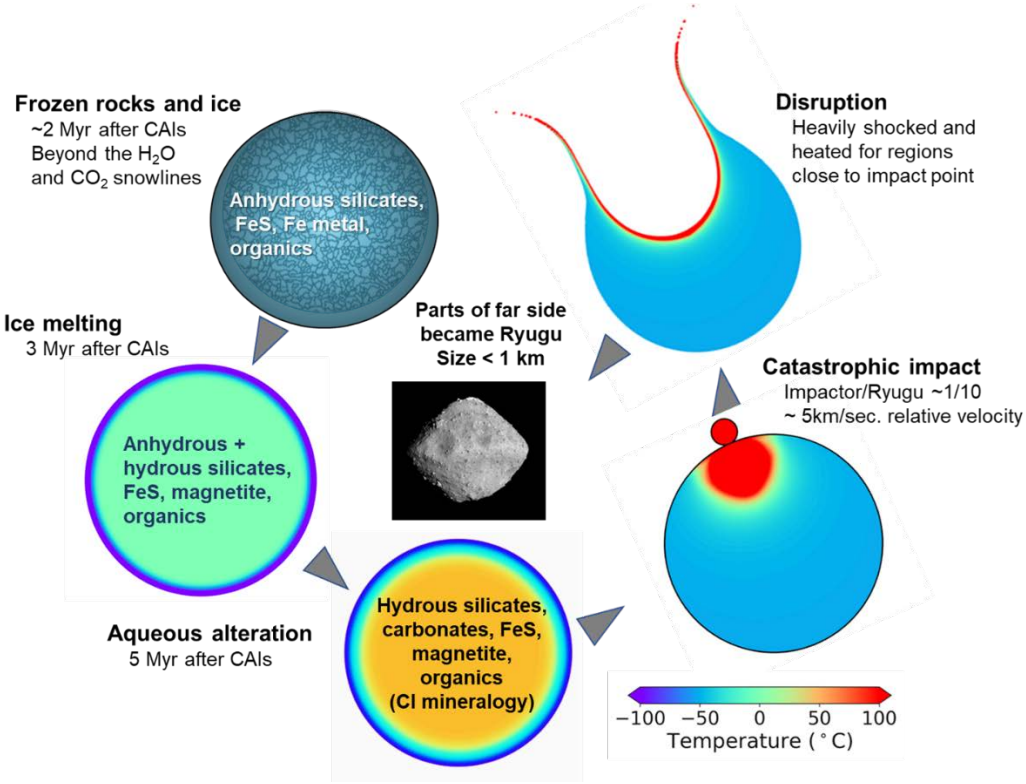

OSIRIS-REx mission

The primary scientific objective of the Origins, Spectral Interpretation, Resource Identification, and Security-Regolith Explorer (OSIRIS-REx) mission (Table 1) is to return and analyze a sample of pristine regolith from a primitive, carbonaceous asteroid to understand the initial stages of planet formation and primordial sources of organics delivered to Earth that may have contributed to life on our planet (Lauretta, 2015). Additional science objectives include: 1) mapping the global chemistry, mineralogy, physical properties, and "geology" of the asteroid, 2) documenting the sampling site down to sub-cm scales for texture, mineralogy, volatile chemistry, and spectral properties, 3) measuring the Yarkovsky effect (which changes the asteroid's orbit over time) on a potentially hazardous asteroid, and 4) directly comparing the integrated global characteristics of a primitive, carbonaceous asteroid to ground-based telescopic data of known asteroids. Here we provide an overview of pre-arrival and remote sensing characteristics of Bennu as well as early sample analysis results.

The asteroid (101955) Bennu (Fig.1A, see spectra in Fig 2AB) was selected as the target

for OSIRIS-REx based on its classification as a B-type asteroid, as well as mission and engineering constraints (Lauretta, 2015). B-type asteroids are broadly characterized by a featureless spectrum with a neutral to bluish spectral slope and low (0.08 - 1.0) visible albedo (Tholen, 1989). Many B-type asteroids appear to be intermediate between asteroids and comets, with evidence for the present-day release of volatiles, suggesting Bennu may contain volatile-rich material. Bennu also meets mission criteria for solar distance, size (~490 m mean diameter), and operational ease of collecting and returning the sample to Earth. Observations made with the Spitzer Space Telescope in 2007 provided an estimate of Bennu's thermal inertia as 310 ±70 J m^2 K^1 $s^{0.5}$, interpreted as suggesting that the regolith would be comprised of fine gravel (sub-cm) optimal for sampling (Emery et al. 2014). Because Bennu's orbit brings it within 0.002 AU of the Earth, it has one of the highest probabilities of impacting the Earth of any known asteroid; as such, Bennu offers an important opportunity to study a potentially hazardous asteroid (PHA).

The OSIRIS-REx spacecraft carries a complement of scientific instruments designed to characterize Bennu as fully as possible to enable sampling site selection, provide context for the returned sample, and better understand carbonaceous Solar System objects. The OSIRIS-REx Camera Suite (OCAMS) consists of three cameras for observing the asteroid at distances ranging from 500,000 km to 2 m (Rizk et al. 2018). One of the cameras, MapCam, allows for mapping of the asteroid at four wavelengths (470, 550, 770, and 860 nm) simulating the Eight-Color Asteroid Survey (ECAS) filter system (b', v, w, and x bands, respectively), allowing for spatially resolved color characterization and direct comparison with Earth-based, multispectral observations. OSIRIS-REx carries two hyperspectral point spectrometers for the identification of minerals, organic chemistry, and measurement of surface temperature. The OSIRIS-REx Visible and Infrared Spectrometer (OVIRS) measures the reflected light spectrum from 0.4 to 4.0 μm (Reuter et al. 2017). The OSIRIS-REx Thermal Emission Spectrometer (OTES) measures the emitted radiance of the asteroid from 5.5 – 50 μm (Christensen et al. 2018). The OSIRIS-REx Laser Altimeter (OLA) provides laser ranging data for the mapping of surface topography and allowing construction of a 3D model of Bennu at the highest resolution recorded on any small body to date (Daly et al. 2017). The Regolith X-ray imaging spectrometer (REXIS) is a student experiment from

the Massachusetts Institute of Technology and Harvard-Smithsonian Center for Astrophysics, designed to map elemental abundances on Bennu (Masterson et al. 2018). OSIRIS-REx also conducts radio science for probing the asteroid's gravity, internal structure, and mass distribution (Scheeres et al. 2016). To collect the crucial regolith sample, OSIRIS-REx employed the Touch and Go Sampling Mechanism (TAGSAM). The TAGSAM is designed to collect a bulk sample consisting of particles up to roughly 2 cm in diameter with a total mass substantially greater than the mission requirement of 60 g. Small, presumably space weathered, surface particles at the uppermost surface are collected by 24 stainless steel contact pads, each ~1.75 cm in diameter (Bierhaus et al. 2018).

Upon arrival at Bennu in 2018, OSIRIS-REx immediately made unexpected discoveries. In one case, the asteroid periodically ejects small particles from a few mm up to 10 cm in size, making it an "active asteroid" (Lauretta and Hergenrother et al. 2019, Chesley et al. 2020). These particles most commonly follow suborbital trajectories (65%), although some complete more than one revolution around the asteroid (20%) and only a small fraction (15%) manage to escape Bennu's gravitational field (Chesley et al. 2020). The ejection events can occur at any local time of day, although most occur in the afternoon and at night (between 12:00 – 24:00 local solar time). Cause(s) of these events that have been considered include meteoroid impacts (Bottke et al. 2020), temperature change-driven sublimation of water ice, or thermal fracturing of rock (Rozitis et al. 2020). Of these, water ice sublimation appears to be the least plausible based on surface temperatures at ejection sites (Rozitis et al. 2020). In another case, resolved imaging of the surface quickly ascertained that the nature of the asteroid's regolith was not as expected; rather than being dominated by cm-scale particles, it is covered in meter-scale rocks and larger boulders with very few areas of regolith dominated by cm-scale particles (Lauretta et al. 2019). However, a few smooth-looking areas up to ~20 m in size are visible, suggesting that smaller particles are present.

In terms of global physical properties, Bennu is extremely dark, with a global geometric albedo of ~4.4% (at 0.55 μm) although there are spatial variations in albedo that result in a range of albedos from ~3.3% to more than 15% (DellaGiustina and Emery et al. 2019). Globally averaged spectral properties include a generally blue slope over 98% of

the surface with the other 2% having a flatter, less blue slope (Barucci et al. 2020). Temperature measurements refined the globally averaged thermal inertia as ~350 ±20 J m^{-2} K^{-1} $s^{-0.5}$ (DellaGiustina and Emery et al. 2019), also with spatial variations ranging from ~180 to 700 J m^{-2} K^{-1} $s^{-0.5}$. These variations in albedo, spectral, and thermophysical properties collectively distinguish two major lithologies (DellaGiustina et al. 2020; Rozitis et al. 2020). Some boulders appear to be breccias that are composed of clasts bound by a dark matrix material and are consistent with impact origins (Walsh et al. 2019). Mass movement affecting the upper ~10 meters of the surface, generally migrating towards the equator, is attributable to gravitational and rotational forces (Jawin et al. 2020). The asteroid exhibits the predicted spinning-top shape with a rotation period of ~4.3 hours and a density of ~1.19 g/cm^3 (Scheeres et al. 2019). This low density, in combination with the asteroid's shape and topography, is consistent with Bennu having a "rubble pile" structure with substantial (~50%) macroporosity, if it is assumed to be comprised of primarily CI- or CM-like carbonaceous chondrite material (Barnouin et al., 2019); therefore, Bennu is probably reaccumulated material produced during a major asteroid collision in the Main Belt, from either the Eulalia or the "new" Polana asteroid family, between 0.7 and 2 Gyr ago (Walsh et al. 2019).

The globally averaged visible to near infrared (VNIR) spectral properties of Bennu (Fig. 2A) provide evidence that Bennu's parent asteroid underwent significant aqueous alteration to produce materials that are like the most aqueously altered carbonaceous chondrites and that the present surface is space weathered. The asteroid's blue slope has been attributed to the presence of fine-particulate magnetite and/or insoluble organic material; it is also commonly associated with larger-particle-size samples and possibly space weathering (Cloutis et al. 2011a; 2011b; Thompson et al. 2019). The dominantly blue spectral slope (0.4 - 0.7 μm) with relatively redder young craters on the surface are consistent with space weathering of a hydrated substrate that becomes increasingly blue with age (e.g., Clark et al. 2023). A spectral feature at 0.55 μm is suggestive of the presence of magnetite (Lauretta et al. 2019). The globally averaged spectrum also exhibits a so-called 3-μm hydration band that is geographically widespread (Hamilton et al. 2019) and relatively invariant in shape and depth (Barucci et al. 2020). The exact position of this feature is ~2.74 ±0.01 μm (Hamilton et al. 2019), consistent with low petrologic type CM chondrites containing abundant Mg-serpentine and "clay" minerals

(Takir et al. 2013). The mean hydrogen content of the water and hydroxyl groups in the hydrated silicates is estimated as 0.71 ±0.16 wt% (Praet et al. 2021). A complex of features around 3.4 μm are indicative of the presence of C-bearing materials, specifically carbonate minerals and organic compounds (Simon et al. 2020; Kaplan et al. 2020). These investigators found that organic signatures do not correlate in location with any other spectral or physical characteristics and variations may be due to differences in abundance, recent exposure, or space weathering. Identified carbonate phases include calcite, Mg-, Fe-bearing carbonate, and dolomite, and in many cases, these phases are associated with cm-wide, m-long relatively bright lineaments in boulders and are interpreted as veins that formed by extensive fluid circulation on spatial scales not evident in carbonaceous chondrites (Kaplan et al. 2020).

Thermal infrared (TIR) spectra exhibit evidence of substantial aqueous alteration on Bennu's parent body as well as evidence for variability in the presence of dust across the surface. The TIR spectra are subdivided into two spectral types, T1 and T2, based on a distinctly different spectral slope between 987 and 814 cm^{-1} (~10.1 and 12.3 μm). This difference is attributed to the variable presence of a minor amount of fine particulate dust rather than a compositional difference, where a ~10 μm thick deposit of particles less than about 50 μm in diameter can produce such a difference in laboratory data (Hamilton et al. 2021; Graff, 2003). Although T1 appears to be the least dusty, neither appears to be entirely free of dust. The spectral types share a common Christiansen feature location at ~1090 cm^{-1} (~9.2 μm), and T1 is dominated by silicate stretching and bending modes with minima near 1000 cm^{-1} (10.0 μm) and 440 cm^{-1} (~22.7 μm), respectively, which are diagnostic of phyllosilicate minerals like the serpentine and saponite found in the most aqueously altered carbonaceous chondrites (Hamilton et al. 2021). Fundamental features of magnetite at 555 and 340 cm^{-1} (~18.0 and 29.4 μm) are observed (Hamilton et al. 2019) and lend credence to the interpretation that the relatively blue spectrum of Bennu at global scales is attributable, in part, to magnetite, analogous to predictions for other B-type asteroids (Yang and Jewitt, 2010). A peak near 528 cm^{-1} (18.9 μm) is diagnostic of the proportions of phyllosilicate and anhydrous minerals (e.g., olivine and pyroxene); based on the presence of this feature, the bulk mineralogy of the surface of Bennu is dominated by Mg-phyllosilicates (>80 vol% of silicates) with less than 10 vol% anhydrous silicates (Hamilton et al. 2021). These

fractions and the presence of magnetite are consistent with petrologic types 1 and 2 on the Van Schmus and Wood (1967) scale or ≤2.4 on the Rubin et al. (2007) scale. The absence of a distinct Mg-OH feature that is observed in carbonaceous chondrites near 625 cm^{-1} (16.0 μm) may be indicative of a non-Mg endmember (Fe-bearing) phyllosilicate composition, modest heating, disorder, a particle size effect, or obscuration by surface dust (Hamilton et al. 2021).

Spectral data also reveal the presence of exogenous materials on Bennu's surface. Relatively bright (13- to 40-sigma above the mean) boulders more than 1.5 m in diameter were observed in OCAMS images in the equatorial to southern latitudes and exhibit a deflection at 1 μm (DellaGiustina et al. 2021). Hyperspectral data in the areas around these boulders exhibit 1- and 2 μm pyroxene features that are inconsistent with chondritic material and instead compare favorably to Howardite-Eucrite-Diogenite (HED) meteorites that are linked to the asteroid 1 Vesta (e.g., Binzel et al. 1993). These boulders, and others found subsequently, likely represent an infall of fragments of Vesta to Bennu or its parent body and imply that if Bennu is a uniform mixture of parent body and S-type materials, the mass of the exogenous materials is equivalent to a sphere 36-40 meters in diameter (DellaGiustina et al. 2021; Le Corre et al. 2021).

Data collected during the asteroid operations phase of the mission were used to select a site on Bennu for sampling. Because of the unexpectedly rugged nature of the asteroid surface, a limited number of locations met requirements for spacecraft navigation and safety as well as having small enough particles to be collected by the TAGSAM. The selected sample site, "Nightingale", is located inside a crater named Hokioi in the northern hemisphere. Nightingale exhibits spectral compositional characteristics consistent with the majority of Bennu, appears to contain both lithologic types, and has a slightly redder normal albedo that is attributed to the crater being young and less space weathered than the majority of the asteroid's surface. The first sampling attempt, on 20 October 2020, was successful and revealed a number of interesting phenomena, which are summarized here and described in detail by Lauretta et al. (2022).

The TAGSAM is mounted on an arm with a telescoping spring; when TAGSAM contacted the surface, nitrogen gas was released, stirring the surface materials and

guiding them into the sampling container. Spacecraft thrusters then maneuvered the spacecraft backwards away from the surface. Data collected during the TAG event show that TAGSAM penetrated 48.8 cm into the subsurface, affirming low-gravity experiments and modeling of regolith materials having little cohesion. Imaging before, during, and after the sample collection showed significant disturbance of surface materials and evidence for differing rock strengths. After sampling, the Hokioi crater region was revisited by the spacecraft instruments to enable analysis of changes in color, composition, topography, and thermophysical properties. The area where sampling occurred was observed to be darker and redder than before the sampling event, with a decrease in reflectance of about 5%, and is interpreted as having exposed even fresher materials enriched in organic compounds. Although several instruments reported the deposition of particulates on their optical surfaces, the surface could still be observed and no significant changes in spectral character or thermal properties at the sampling site were identified.

In the days after sample collection, imaging of the TAGSAM confirmed the presence of a substantial amount of material in the collection chamber, as well as particles captured in the stainless steel, hook-and-loop contact pads (designed to sample the uppermost, space-weathered surface). Imaging also revealed that small stones lodged between the mylar flap closure and the sample chamber were allowing the escape of sample material. The last estimate of sample mass prior to stowage of TAGSAM, eight days after sampling, was 250 ± 101g, a loss of approximately 67 g since a mass estimate made two days after sampling (Lauretta et al. 2022).

The Sample Return Capsule (SRC) successfully landed at the Utah Test and Training Range (UTTR) on 24 September 2023 and, within hours, was transported to a temporary clean room facility at UTTR before being flown to Houston, TX and the clean curation facility at NASA Johnson Space Center (JSC). The opening of the SRC, disassembly of the TAGSAM, mass measurement and containerization of sample material, and processing and allocations of sample material for scientific analysis all occur at JSC. The TAGSAM head after removal from the SRC is shown in Figure 13. The total mass returned was determined to be 121.6 g, more than double the mission's requirement to return 60 g (Lauretta and Connolly et al. 2024), but less than the

minimum mass (including uncertainty) of 149 g determined from the in-situ measurement. Because of the observed escape of material, the TAGSAM was stowed earlier than planned and the method used for the in-situ estimation differed from the planned sample mass measurement approach (Ma et al. 2021). The difference between the in situ and final (JSC) mass measurements may be attributable to sample loss during stowage (where the estimate of 2.2 g min^{-1} represented a lower bound; Lauretta et al. 2022), unforeseen factors affecting the spacecraft's measurement accuracy, or both.

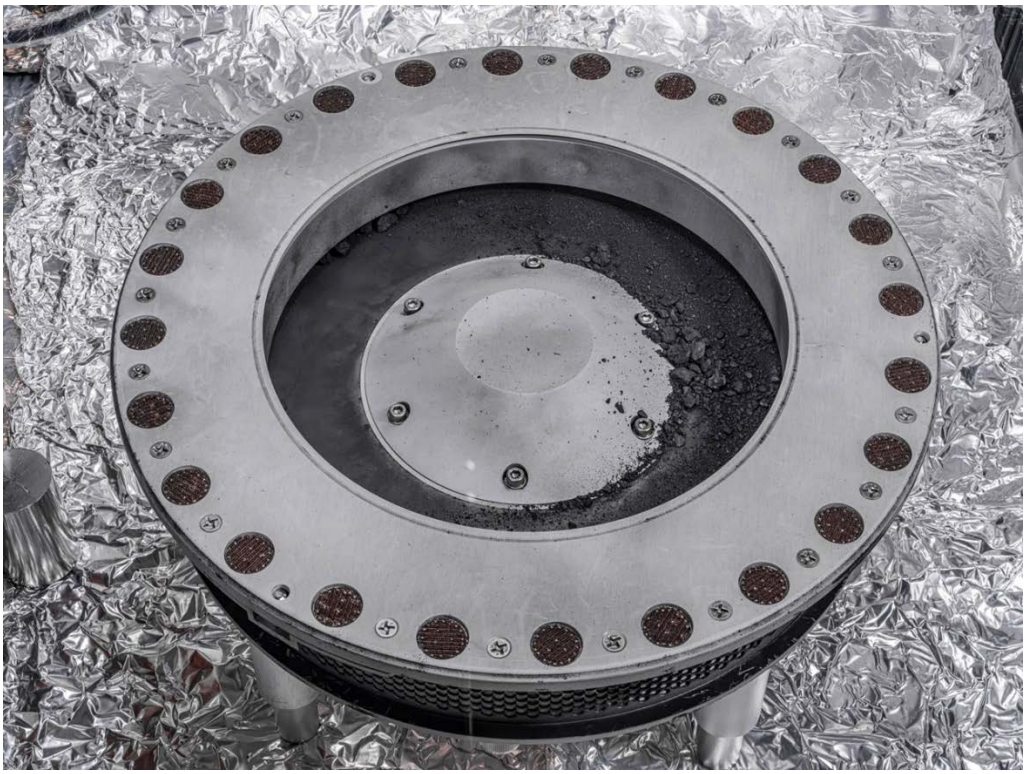

Fig. 13. Sample container of OSIRIS-REx Touch-and-Go Sample Acquisition Mechanism. Contact pads around ring (between screws) are ~17 mm in diameter. In the inner ring, small pebbles can be seen at upper left holding open the mylar flap. Pebbles and fine particulates are visible on top of the mylar flap at right. The presence of coarse and fine particles confirms remote sensing interpretations. Image source: https://www.asteroidmission.org/?latest-news=nasas-osiris-rex-achieves-sample-mass-milestone

The OSIRIS-REx science team developed a hypothesis-driven Sample Analysis Plan (Lauretta et al. 2023) There are 12 top-level hypotheses that are fundamental to the

mission science and relate to remote observations of Bennu prior to and during the operations phase of the mission and to our understanding of carbonaceous chondrites and the formation and evolution of the Solar System. The 12 hypotheses (and their sub-hypotheses) fall into five broad categories: 1) the fundamental nature of Bennu, 2) the pre-accretionary environment and formation of Bennu's parent asteroid, 3) the scattering of Bennu's parent body into the inner Solar System, geological activity, surface modification, and catastrophic disruption, 4) Bennu's formation, dynamical, and geological evolution, and 5) sample collection operations and Earth return. Published results to date from the earliest Bennu sample analyses focus on testing the first hypothesis (and its five sub-hypotheses) in the Sample Analysis Plan, which posits that remote sensing observations of Bennu accurately characterized its mineral, chemical and physical properties. In fact, the sample has both validated observations made at the asteroid and revealed new information; the summary below is derived from Lauretta et al. (2024).

Particles in the returned sample (Figure 14) exhibit morphologies (angular and hummocky) that resemble and may be related to the morphologies of boulders observed on the asteroid's surface and likely represent the two lithologies identified there. Particles with a mottled appearance may be related to bright veins observed in some boulders. These three particle types exhibit different densities, where the hummocky stones are the least dense (1.55 ±0.07 g/cm^3), followed by the angular stones (1.69 ±0.04 g/cm^3), and the mottled stones being the densest (1.77 ±0.04 g/cm^3). Preliminary assessment of how these density values translate to a macroporosity for Bennu are presented by Ryan et al. (2024). Those investigators determined Bennu's macroporosity is somewhat lower (20–33%) than prior estimates (25–50%, above); but do not change the interpretation that Bennu is a rubble pile asteroid. Although the albedo of Bennu materials at ~1 μm is like that observed at Bennu, the spectrum of aggregated particles from 0.4 to 2.5 μm is considerably redder than global average Bennu; this may represent a lesser degree of space weathering, particle size effects, or a textural effect, but more analyses are needed to definitively establish the origin of this difference.

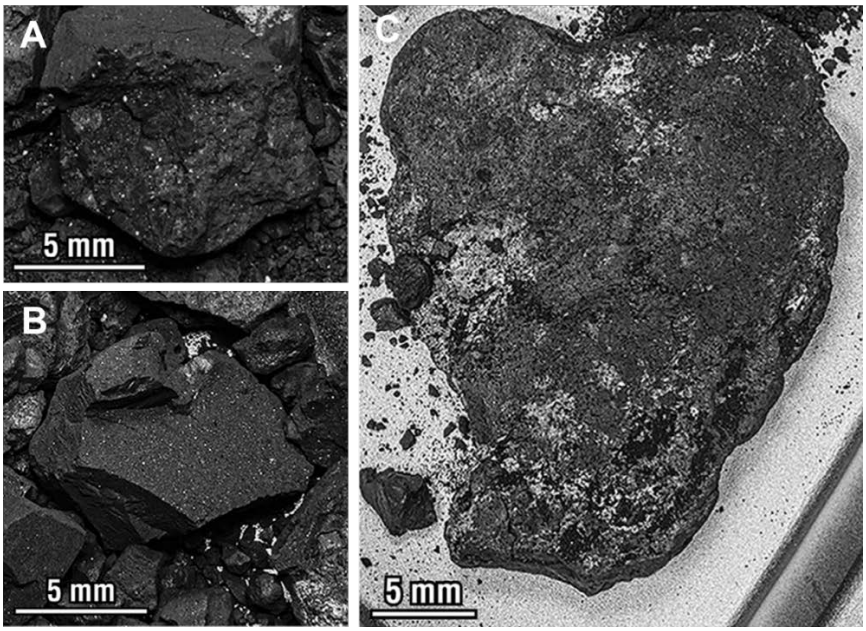

Fig. 14. Examples of stone morphologies observed in Bennu sample. (A) hummocky, (B) angular, and (C) mottled. After Lauretta et al. (2024).

The material returned from Bennu is comprised dominantly of hydrous minerals (phyllosilicates) with lesser amounts of magnetite and carbonate as predicted. Indirectly inferred from remote sensing was the presence of Fe,Ni-sulfides, which are also present. Measurements of hydrogen content range from 0.86–0.98 wt% (including uncertainties), which just overlaps (at the low end) the remote sensing-derived value of 0.71 ± 0.16 wt%); the variance may be attributable to the differences in shape and position between the 3-µm hydration band in asteroid and sample spectra (Lauretta and Connolly et al. 2024; Praet et al., 2021). Anhydrous phases such as olivine and pyroxene were not observed and were expected to be present at less than 10 vol%; forsteritic olivine and low-Ca pyroxene are found in the sample at generally minor abundances along with spinel, chromite, and ilmenite. The identification in the sample of Mg,Na- and Ca-phosphates at trace abundances and on particle surfaces was not anticipated and its origin as part of an evaporite sequence has since been described in detail (McCoy and Russell et al. 2025); whether phosphates are identifiable in Bennu spectra is a subject of further study.

No exogenic materials resembling HED meteorites have been identified in the sample yet, but there are strong similarities with aqueously altered carbonaceous chondrites,

specifically the CI group and Tarda (C2-ung), in terms of modal mineralogy. Bulk elemental analysis of material from inside and outside the TAGSAM exhibit slightly different values for 10 elements that are known to be mobile and could support the open hydrothermal system proposed based on carbonate-bearing veins in Bennu boulders. Organic compounds are present as expected, with a high (relative to typical carbonaceous chondrites) total C content of 4.5 - 4.7 wt%. The samples are volatile rich, containing more carbon, nitrogen, and ammonia than most meteorites or samples of Ryugu (Glavin et al. 2025). Analysis of organic nanoglobules and PAHs does not show any indication of significant thermal alteration. Oxygen isotope analysis places Bennu near the chemically primitive CI and CY chondrites and Ryugu, but with a slightly higher $\Delta^{17}O$ value. Presolar materials (SiC and graphite) have been identified at abundances consistent with other unheated chondrite samples.

Bennu materials exhibit physical properties that suggest they may differ from carbonaceous meteorites, such as higher porosity and lower density. The bulk density of hummocky particles is relatively low, like that of Orgueil (CI1) and supports the idea that materials like these are unable to withstand impact with the Earth's atmosphere.

Overall, the materials returned from asteroid Bennu confirm predictions from ground-based telescopic and orbital remote sensing of a highly aqueously altered, C-enriched asteroid. The identification of hydrated phosphates indicates a more complex fluid chemistry than would otherwise be inferred. Although preliminary analysis of particles suggests they can be related to boulder types on Bennu that are thought to have different physical properties, more data are required to be certain of these links and produce updated values of properties such as asteroid macroporosity. Although the sampled surface of Bennu is extensively aqueously altered, it still retains some components from the protoplanetary disk. Even with the overall success of remote sensing observations, laboratory observations of the returned sample reveal detailed characteristics that would not have been known otherwise and demonstrates the extraordinary value of having samples of planetary bodies to help understand their complex histories.

MMX mission

Visible to near-infrared reflectance spectra of Phobos and Deimos (Fig. 2A) are similar

in reflectance and shape to those of D-type and T-type asteroids, which are probably made up of primitive carbonaceous chondrite-like material (Rivkin et al. 2002; Fraeman et al. 2012). The size of the two moons is also in the range of asteroids (Table 1E), and therefore they are thought to be captured asteroids. If the moons are captured asteroids, then they might have formed beyond the snowline near the young Jupiter and transferred to the inner region across the snowline. If this is valid, then Phobos and Deimos may be representatives of carriers that delivered water and organics to the inner planets. There are many hypotheses for the origin of the two moons. They are divided into two major models, each of which predicts an expected material composition of the moons; one is chondritic, and the other is non-chondritic. The major model of non-chondritic composition is giant impact model (e. g., Craddock 2011; Rosenblatt et al. 2016; Hyodo et al. 2017) in which a small body collided with Mars, making a large crater on the Mars and a dust disk around Mars that consisted of impact ejecta. The two moons are expected to have formed by accretion of the disk material and thus they are small and have near-circular equatorial orbits (Rosenblatt et al. 2016; Hyodo et al. 2017). Temperature, cooling rates, and chemical composition of the material in the disk are estimated based on thermodynamic condensation models (Pignatale et al. 2018).

The MMX mission aims to determine the origin of the Martian moons based on the remote sensing observation of Phobos and Deimos for about three years and the laboratory analysis of Phobos returned samples (Kuramoto et al. 2021). It is important to confirm from MMX's remote sensing spectroscopic observations of the whole surface and the sample collection sites that the samples to be brought back to Earth are representative material of Phobos (or Phobos-indigenous materials). The key observations to constrain the origin of Phobos and Deimos are: 1. to estimate the elemental abundances of Phobos globally (Laurence et al. 2021) and determine whether it is chondritic or non-chondritic composition (including Martian components or not); 2. to perform global high-spatial resolution spectroscopy to obtain visible and near-infrared reflectance spectra to determine if hydrous minerals are ubiquitously distributed on Phobos and Deimos (Barucci et al. 2021), and 3. to perform a variety of analyses on returned Phobos samples mirroring those done for the Hayabusa2 returned samples in order to determine the source material of Phobos and formation and alteration conditions based on mineralogy and isotopic composition (Fujiya et al. 2021). If these observations and analyses are successful, we should be able to determine the origin and

formation process of the Martian moons within a few years from the sample return expected in 2031.

Acknowledgement: This work was supported by JSPS KAKENHI Grant Number 24H00259 to TN. CE is supported by CNRS and the Centre National d'Etudes Spatiales (CNES) in the frame of the MIAMI-H2 project. VEH is supported by NASA under contract NNM10AA11C issued through the New Frontiers Program. AAF is supported by NASA's MMX Participating Scientist Program, and carried out research at the Jet Propulsion Laboratory, California Institute of Technology under a contract with NASA (80NM0018D0004).

References

Abe M, Takagi Y, Kitazato K et al (2006) Near-infrared spectral results of asteroid Itokawa from the Hayabusa spacecraft. Science 312:1334-1338. https://doi.org/10.1126/science.1125718

Abe S, Mukai T, Hirata N et al (2006) Mass and local topography measurements of Itokawa by Hayabusa. Science 312:1344-1347. https://doi.org/10.1126/science.1126272

Aléon-Toppani A, Brunetto R, Dionnet Z et al (2024) Correlated IR-SEM-TEM studies of three different grains from Ryugu: From the initial material to post-accretional processes. Geochimica et Cosmochimica Acta. https://doi.org/10.1016/j.gca.2024.02.006

Allen CW, Cox AN (2000) *Allen's astrophysical quantities*. Springer Science & Business Media, pp. 294.

Amano K, Matsuoka M, Nakamura T et al (2023) Reassigning CI chondrite parent bodies based on reflectance spectroscopy of samples from carbonaceous asteroid Ryugu and meteorites. Science advances 9:eadi3789. https://doi.org/10.1126/sciadv.adi3789

Aponte, J.C., Dworkin, J.P., Glavin, D.P., Elsila, J.E., Parker, E.T., McLain, H.L., Naraoka, H., Okazaki, R., Takano, Y., Tachibana, S., Dong, G., Zeichner, S.S., Eiler, J.M., Yurimoto, H., Nakamura, T., Yabuta, H., Terui, F., Noguchi, T., Sakamoto, K., Yada, T., Nishimura, M., Nakato, A., Miyazaki, A., Yogata, K., Abe, M., Okada, T., Usui, T., Yoshikawa, M., Saiki, T., Tanaka, S., Nakazawa, S., Tsuda, Y., Watanabe, S., The Hayabusa2-initial-analysis SOM team, The Hayabusa2-initial-analysis core team (2023) PAHs, hydrocarbons, and dimethylsulfides in Asteroid Ryugu samples A0106 and C0107 and the Orgueil (CI1) meteorite. Earth, Planets and Space 75: 28.

https://doi.org/10.1186/s40623-022-01758-4

Arakawa M, Saiki T, Wada K et al (2020) An artificial impact on the asteroid (162173) Ryugu formed a crater in the gravity-dominated regime. Science 368:67-71. https://doi.org/10.1126/science.aaz1701

Barnes JJ, Haenecour P, Smith LR et al (2024) Coordinated Analysis of Phosphates in Samples From Asteroid (101955) Bennu. In 55th Lunar and Planetary Science Conference (LPSC). Lunar and Planetary Institute. https://ntrs.nasa.gov/citations/20240000339

Barnouin, O. S., M. G. Daly, E. E. Palmer, R. W. Gaskell, J. R. Weirich, C. L. Johnson, M. M. Al Asad, J. H. Roberts, M. E. Perry, H. C. M. Susorney, R. T. Daly, E. B. Bierhaus, J. A. Seabrook, R. C. Espiritu, A. H. Nair, L. Nguyen, G. A. Neumann, C. M. Ernst, W. V. Boynton, M. C. Nolan, C. D. Adam, M. C. Moreau, B. Rizk, C. Y. Drouet D'Aubigny, E. R. Jawin, K. J. Walsh, P. Michel, S. R. Schwartz, R. L. Ballouz, E. M. Mazarico, D. J. Scheeres, J. W. McMahon, W. F. Bottke, S. Sugita, N. Hirata, N. Hirata, S. i. Watanabe, K. N. Burke, D. N. DellaGiustina, C. A. Bennett, D. S. Lauretta and O.-R. Team (2019). "Shape of (101955) Bennu indicative of a rubble pile with internal stiffness." Nature Geoscience **12**(4): 247-252. https://doi.org/10.1038/s41561-019-0330-x

Barucci MA, Hasselmann PH, Praet A, Fulchignoni M, Deshapriya JDP, Fornasier S, Merlin F, Clark BE, Simon AA, Hamilton VE, Emery JP, Howell ES, Brucato JR, Cloutis EA, Zou XD, Li J-Y, Michel P, Ferrone S, Poggiali G, Reuter DC, DellaGiustina DN, Lauretta DS (2020) OSIRIS-REx spectral analysis of (101955) Bennu by multivariate statistics. Astronomy & Astrophysics 637:L4. https://doi.org/10.1051/0004-6361/202038144

Barucci MA, Reess JM, Bernardi P et al (2021) MIRS: an imaging spectrometer for the MMX mission; Earth, Planets and Space 73; 1-28. https://doi:10.1186/s40623-021-01423-2

Bierhaus EB, Clark BC, Harris JW, Payne KS, Dubisher RD, Wurts EW, Hund RA, Kuhns RM, Linn TM, Wood JL, May AJ, Dworkin JP, Beshore E, Lauretta DS, the OSIRIS-REx Team (2018) The OSIRIS-REx spacecraft and the Touch-and-Go Sample Acquisition Mechanism (TAGSAM). Space Science Reviews 2014:107. https://doi.org/10.1007/s11214-018-0521-6

Binzel RP and Xu S (1993) Chips off of asteroid 4 Vesta: Evidence for the parent body of basaltic achondrites meteorites. Science 260:186-191. https://doi.org/10.1126/science.260.5105.18

Binzel RP, Bus SJ, Burbine TH et al (1996) Spectral properties of near-Earth asteroids: Evidence for sources of ordinary chondrite meteorites. Science 273:946-948. https://doi.org/10.1126/science.273.5277.946

Bonal, L., Quirico, E., Montagnac, G., Komatsu, M., Kebukawa, Y., Yabuta, H.,

Amano, K., Barosch, J., Bejach, L., Cody, G.D., Dartois, E., Dazzi, A., De Gregorio, B., Deniset-Besseau, A., Duprat, J., Engrand, C., Hashiguchi, M., Kamide, K., Kilcoyne, D., Martins, Z., Mathurin, J., Mostefaoui, S., Nittler, L., Ohigashi, T., Okumura, T., Remusat, L., Sandford, S., Shigenaka, M., Stroud, R., Suga, H., Takahashi, Y., Takeichi, Y., Tamenori, Y., Verdier-Paoletti, M., Yamashita, S., Nakamura, T., Naraoka, H., Noguchi, T., Okazaki, R., Yurimoto, H., Tachibana, S., Abe, M., Miyazaki, A., Nakato, A., Nakazawa, S., Nishimura, M., Okada, T., Saiki, T., Sakamoto, K., Tanaka, S., Terui, F., Tsuda, Y., Usui, T., Watanabe, S., Yada, T., Yogata, K., Yoshikawa, M. (2024) The thermal history of Ryugu based on Raman characterization of Hayabusa2 samples. Icarus 408, 115826. https://doi.org/10.1016/j.icarus.2023.115826

Bottke WF, Moorhead AV, Connolly, Jr HC, Hergenrother CW, Molaro JL, Michel P, Nolan MC, Schwartz SR, Vokrouhlický D, Walsh KJ, Lauretta DS (2020) Meteoroid impacts as a source of Bennu's particle ejection events. Journal of Geophysical Research - Planets 125: e2019JE006282. https://doi.org/10.1029/2019JE006282

Britt DT, Tholen DJ, Bell JF et al (1992) Comparison of asteroid and meteorite spectra: Classification by principal component analysis. Icarus 99:153-166. https://doi.org/10.1016/0019-1035(92)90179-B

Brownlee DE, Horz F, Newburn RL (2004) Surface of young Jupiter family comet 81P/Wild 2: View from the Stardust spacecraft. Science 304:1764-1769. https://doi.org/10.1126/science.1097899

Brownlee DE, Tsou P, Anderson JD et al (2003) Stardust: Comet and interstellar dust sample return mission. Journal of Geophysical Research: Planets 108. https://doi.org/10.1029/2003JE002087

Bus SJ, Binzel RP (2002a) Phase II of the small main-belt asteroid spectroscopic survey: The observations. Icarus 158:106-145. https://doi.org/10.1006/icar.2002.6857

Bus SJ, Binzel RP (2002b) Phase II of the small main-belt asteroid spectroscopic survey: A feature-based taxonomy. Icarus 158:146-177. https://doi.org/10.1006/icar.2002.6856

Craddock RA (2011) Are Phobos and Deimos the result of a giant impact? Icarus 211; 1150-1161. https://doi: 10.1016/j.icarus.2010.10.023

Che S and Zega TJ (2023) Hydrothermal fluid activity on asteroid Itokawa. Nature Astronomy 7.9: 1063-1069.

Chesley SR, French AS, Davis AB, Jacobson RA, Brozović M, Farnocchia D, Selznick S, Liounis AJ, Hergenrother CW, Moreau MC, Pelgrift J, Lessac-Chenen E, Molaro JL, Park RS, Rozitis B, Scheeres DJ, Takahashi Y, Vokrouhlický D, Wolner CWV, Adam C, Bos BJ, Christensen EJ, Emery JP, Leonard JM, McMahon JW, Nolan MC, Shelly FC, Lauretta DS (2020) Trajectory estimation for particles observed in the

vicinity of (101955) Bennu. Journal of Geophysical Research - Planets 125:e2019JE006363. https://doi.org/10.1029/2019JE006363

Christensen PR, Hamilton VE, Mehall GL, Pelham D, O'Donnell W, Anwar S, Bowles H, Chase S, Fahlgren J, Farkas Z, Fisher T, James O, Kubik I, Lazbin I, Miner M, Rassas M, Schulze L, Shamordola K, Tourville T, West G, Woodward R, Lauretta D (2018) The OSIRIS-REx Thermal Emission Spectrometer (OTES) instrument. Space Science Reviews 214:87. https://doi.org/10.1007/s11214-018-0513-6

Clark, BE et al (2023) Overview of the search for signs of space weathering on the low-albedo asteroid (101955) Bennu. Icarus 400:115563. https://doi.org/10.1016/j.icarus.2023.115563

Cloutis EA, Hiroi T, Gaffey MJ, Alexander CMO'D, Mann P (2011a) Spectral reflecctance properties of carbonacous chondrites: 1. CI chondrites. Icarus 212:180-209. https://10.1016/j.icarus.2010.12.009

Cloutis EA, Hudon P, Hiroi T, Gaffey MJ, Mann P (2011b) Spectral reflectance properties of carbonaceous chondrites: 2. CM chondrites. Icarus 216:309-346. https://10.1016/j.icarus.2011.09.009

Cloutis EA, Pietrasz VB, Kiddell C (2018) Spectral reflectance "deconstruction" of the Murchison CM2 carbonaceous chondrite and implications for spectroscopic investigations of dark asteroids. Icarus 305:203-224. https://doi.org/10.1016/j.icarus.2018.01.015

Daly MG, Barnouin OS, Dickinson C, Seabrook J, Johnson CL, Cunningham G, Haltigin T, Gaudreau D, Brunet C, Aslam I, Taylor A, Bierhaus EB, Boynton W, Nolan M, Lauretta DS (2017) The OSIRIS-REx Laser Altimeter (OLA) Investigation and Instrument. Space Science Reviews 212:899–924. https://doi.org/10.1007/s11214-017-0375-3

Dartois, E., Kebukawa, Y., Yabuta, H., Mathurin, J., Engrand, C., Duprat, J., Bejach, L., Dazzi, A., Deniset-Besseau, A., Bonal, L., Quirico, E., Sandt, C., Borondics, F., Barosch, J., Cody, G.D., Gregorio, B.T.D., Hashiguchi, M., Kilcoyne, D.A.L., Komatsu, M., Martins, Z., Matsumoto, M., Montagnac, G., Mostefaoui, S., Nittler, L.R., Ohigashi, T., Okumura, T., Remusat, L., Sandford, S., Shigenaka, M., Stroud, R., Suga, H., Takahashi, Y., Takeichi, Y., Tamenori, Y., Verdier-Paoletti, M., Yamashita, S., Nakamura, T., Morita, T., Kikuiri, M., Amano, K., Kagawa, E., Noguchi, T., Naraoka, H., Okazaki, R., Sakamoto, K., Yurimoto, H., Abe, M., Kamide, K., Miyazaki, A., Nakato, A., Nakazawa, S., Nishimura, M., Okada, T., Saiki, T., Tachibana, S., Tanaka, S., Terui, F., Tsuda, Y., Usui, T., Watanabe, S., Yada, T., Yogata, K., Yoshikawa, M. (2023) Chemical composition of carbonaceous asteroid Ryugu from synchrotron spectroscopy in the mid- to far-infrared of Hayabusa2-

returned samples. Astronomy &Astrophysics 671, A2. https://doi.org/10.1051/0004-6361/202244702

Davidsson BJ, Gutiérrez PJ (2006) Non-gravitational force modeling of Comet 81P/Wild 2: I. A nucleus bulk density estimate. Icarus 180:224-242. https://doi.org/10.1016/j.icarus.2005.07.023

De Gregorio, B.T., Cody, G.D., Stroud, R.M., Kilcoyne, A.L.D., Sandford, S., Le Guillou, C., Nittler, L.R., Barosch, J., Yabuta, H., Martins, Z., Kebukawa, Y., Okumura, T., Hashiguchi, M., Yamashita, S., Takeichi, Y., Takahashi, Y., Wakabayashi, D., Engrand, C., Bejach, L., Bonal, L., Quirico, E., Remusat, L., Duprat, J., Verdier-Paoletti, M., Mostefaoui, S., Komatsu, M., Mathurin, J., Dazzi, A., Deniset-Besseau, A., Dartois, E., Tamenori, Y., Suga, H., Montagnac, G., Kamide, K., Shigenaka, M., Matsumoto, M., Enokido, Y., Yoshikawa, M., Saiki, T., Tanaka, S., Terui, F., Nakazawa, S., Usui, T., Abe, M., Okada, T., Yada, T., Nishimura, M., Nakato, A., Miyazaki, A., Yogata, K., Yurimoto, H., Nakamura, T., Noguchi, T., Okazaki, R., Naraoka, H., Sakamoto, K., Tachibana, S., Watanabe, S., Tsuda, Y. (2024) Variations of Organic Functional Chemistry in Carbonaceous Matter from the Asteroid 162173 Ryugu. Nature Communications, in press.

DellaGiustina DN and Emery JP, et al. (2019) Properties of rubble pile asteroid (101955) Bennu from OSIRIS-REx imaging and thermal analysis. Nature Astronomy 4:341-351. https://doi.org/10.1038/s41550-019-0731-1

DellaGiustina DN, et al. (2020) Variations in color and reflectance on the surface of asteroid (101955) Bennu. Science 370:eabc3660. https://doi.org/10.1126/science.abc3660

DellaGiustina DN et al (2021) Exogenic basalt on asteroid (101955) Bennu. Nature Astronomy 5:31-38. https://doi.org/10.1038/s41550-020-1195-z

DeMeo FE, Binzel RP, Slivan SM (2009) An extension of the Bus asteroid taxonomy into the near-infrared. Icarus 202:160-180. https://doi.org/10.1016/j.icarus.2009.02.005

DeMeo FE, Burt BJ, Marsset M et al (2022) Connecting asteroids and meteorites with visible and near-infrared spectroscopy. Icarus 380:114971. https://doi.org/10.1016/j.icarus.2018.01.015

Demura H, Kobayashi S, Nemoto E et al (2006). Pole and global shape of 25143 Itokawa. Science 312:1347-1349. https://doi.org/10.1126/science.1126574

Dionnet Z, Rubino S, Aléon-Toppani A (2023) Three-dimensional multiscale assembly of phyllosilicates, organics, and carbonates in small Ryugu fragments. Meteoritics & Planetary Science. https://doi.org/10.1111/maps.14068

Duxbury TC, Newburn RL, Brownlee DE (2004) Comet 81P/Wild 2 size, shape, and

orientation. Journal of Geophysical Research: Planets 109. https://doi.org/10.1029/2004JE002316

Ebihara M, Sekimoto S, Shira N et al (2011) Neutron activation analysis of a particle returned from asteroid Itokawa. Science 333:1119-1121. https://doi.org/10.1126/science.1207865

Emery JP, Fernández YR, Kelley MSP, Warden KT (nèe Crange), Hergenrother C, Lauretta DS, Drake MJ, Campins H, and Ziffer J (2014) Thermal infrared observations and thermophysical characterization of OSIRIS-REx target asteroid (101955) Bennu. Icarus 234:17–35. https://dx.doi.org/10.1016/j.icarus.2014.02.005

Ernst CM, Daly RT, Gaskell RW (2023) High-resolution shape models of Phobos and Deimos from stereophotoclinometry. Earth, Planets and Space 75:103. https://doi.org/10.1186/s40623-023-01814-7

Fraeman AA, Arvidson RE, Murchie SL et al (2012) Analysis of disk-resolved OMEGA and CRISM spectral observations of Phobos and Deimos. Journal of Geophysical Research: Planets 117. https://doi.org/10.1029/2012JE004137

Fujiwara A, Kawaguchi J, Yeomans DK et al (2006) The rubble-pile asteroid Itokawa as observed by Hayabusa. Science 312:1330-1334. https://doi.org/10.1126/science.1125841

Fujiya W, Furukawa Y, Sugahara H et al (2021) Analytical protocols for Phobos regolith samples returned by the Martian Moons eXploration (MMX) mission. Earth, Planets and Space 73; 1-24. https://doi: 10.1186/s40623-021-01438-9

Fujiya W, Kawasaki N, Nagashima K et al (2023) Carbonate record of temporal change in oxygen fugacity and gaseous species in asteroid Ryugu. Nature Geoscience 16:675-682. https://www.nature.com/articles/s41561-023-01226-y

Glavin, D. P., Dworkin, J. P., Alexander, C. M. O'D., Aponte, J. C., Baczynski, A.A., Barnes, J. J., Bechtel, H. A., Berger, E. L., Burton, A. S., Caselli, P., Chung, A. H., Clemett, Simon J., Cody, G. D., Dominguez, G., Elsila, J. E., Farnsworth, K. K., Foustoukos, D. I., Freeman, K. H., Furukawa, Y., Gainsforth, Z., Graham, H. V., Grassi, T., Giuliano, B. M., Hamilton, V. E., Haenecour, P., Heck, P. R., Hofmann, A. E., House, C. H., Huang, Y., Kaplan, H. H., Keller, L. P., Kim, B., Koga, T., Liss, M., McLain, H. L., Marcus, M. A., Matney, M., McCoy, T. J., McIntosh, O. M., Mojarro, A., Naraoka, H., Nguyen, A. N., Nuevo, M., Nuth, J. A., Oba, Y., Parker, E. T., Peretyazhko, T. S., Sandford, S.A., Santos, E., Schmitt-Kopplin, P., Seguin, F., Simkus, D. N., Shahid, A., Takano, Y., Thomas-Keprta, K. L., Tripathi, H., Weiss, G., Zheng, Y., Lunning, N. G., Righter, K., Connolly, H. C., Lauretta, D. S. (2025), Abundant ammonia, nitrogen-rich soluble organic matter in samples from asteroid (101955) Bennu, *Nature Astronomy*, *9*, 199-210, doi:10.1038/s41550-024-02472-9.

Graff TG (2003) Effects of dust coatings on visible, near-infrared, thermal emission and Mössbauer spectra: Implications for mineralogical remote sensing of Mars. MS Thesis, Arizona State University.

Guo Y, Farquhar RW (2008) New Horizons mission design. Space science reviews 140:49-74. https://doi.org/10.1007/s11214-007-9242-y

Hamilton VE, Simon AA, Christensen PR, Reuter DC, Clark BE, Barucci MA, Bowles NE, Boynton WV, Brucato JR, Coutis EA, Connolly, JR HC, Donaldson Hanna KL, Emery JP, Enos HL, Fornasier S, Haberle CW, Hanna RD, Howell ES, Kaplan HH, Keller LP, Lantz C, Li J-Y, McCoy TJ, Merlin F, Nolan MC, Praet A, Rozitis B, Sandford SA, Schrader DL, Thomas CA, Zou X-D, Lauretta DS, the OSIRIS-REx Team (2019) Evidence for widespread hydrated minerals on asteroid (101955) Bennu. Nature Astronomy 3:332-340. https://doi.org/10.1038/s41550-019-0722-2

Hamilton VE, Christensen PR, Kaplan HH, Haberle CW, Rogers AD, Glotch TD, Breitenfeld LB, Goodrich CA, Schrader DL, McCoy TJ, Lantz C, Hanna RD, Simon AA, Brucato JR, Clark BE, Lauretta DS (2021) Evidence for limited compositional and particle size variation on asteroid (101955) Bennu from thermal infrared spectroscopy. Astronomy & Astrophysics 650:A120. https://doi.org/10.1051/0004-6361/202039728

Hamilton VE, Keller LP, Haenecour P (2024) Mineralogy of Bennu From Spectral Analysis of the Sample Returned By OSIRIS-REx. In 55th Lunar and Planetary Science Conference.

Hirabayashi M, Hirata N, Kamata S et al (2021) Hayabusa2 Extended Mission: Rendezvous with 1998 KY26, one of the most common but unexplored near-Earth asteroids. Copernicus Meetings. https://doi.org/10.5194/epsc2021-442

Hiroi T, Zolensky ME, Pieters CM et al (1996) Thermal metamorphism of the C, G, B, and F asteroids seen from the 0.7 μm, 3 μm, and UV absorption strengths in comparison with carbonaceous chondrites. Meteorit. Planet. Sci. 31:321–327. https://doi.org/10.1111/j.1945-5100.1996.tb02068.x

Hiroi T, Abe M, Kitazato K et al (2006) Developing space weathering on the asteroid 25143 Itokawa. Nature 443:56-58. https://www.nature.com/articles/nature05073

Hopp T, Dauphas N, Abe Y et al (2022) Ryugu's nucleosynthetic heritage from the outskirts of the Solar System. Science advances 8:eadd8141. https://doi.org/10.1126/sciadv.add8141

Hyodo R, Genda H, Charnoz S, Rosenblatt P (2017) On the impact origin of Phobos and Deimos. I. Thermodynamic and physical aspects. The Astrophysical Journal 845; 125. https://doi.org/10.3847/1538-4357/aa81c4

Ishizaki T, Nagano H, Tanaka S (2023) Measurement of microscopic thermal diffusivity

distribution for Ryugu sample by infrared lock-in periodic heating method. International Journal of Thermophysics 44:51. https://doi.org/10.1007/s10765-023-03158-6

Ito M, Tomioka N, Uesugi M et al (2022) A pristine record of outer Solar System materials from asteroid Ryugu's returned sample. Nature Astronomy 6:1163-1171. https://www.nature.com/articles/s41550-022-01745-5

Jawin ER, Walsh KJ, Barnouin OS, McCoy TJ, Ballouz R-L, DellaGiustina DN, Connolly, Jr HCC, Marshall J, Beddingfield C, Nolan MC, Molaro JL, Bennett CA, Scheeres DJ, Daly MG, Al Asad M, Daly RT, Bierhaus EB, Susorney HCM, Kaplan HH, Enos HL, Lauretta DS (2020) Global patterns of recent mass movement on asteroid (101955) Bennu. Journal of Geophysical Research - Planets 125:e2020JE006475. https://doi.org/10.1029/2020JE006475

Jin Z, Maitrayee B (2019) New clues to ancient water on Itokawa. Science Advances 5.5:eaav8106. https://doi.org/10.1126/sciadv.aav8106

Jourdan F, Timms NE, Eroglu E et al (2017) Collisional history of asteroid Itokawa. Geology 45:819-822. https://doi.org/10.1130/G39138.1

Jourdan F, Timms NE, Nakamura T et al (2023) Rubble pile asteroids are forever. Proceedings of the National Academy of Sciences 120:e2214353120. https://doi.org/10.1073/pnas.2214353120

Kameda S, Ozaki M, Enya K et al (2021) Design of telescopic nadir imager for geomorphology (TENGOO) and observation of surface reflectance by optical chromatic imager (OROCHI) for the Martian Moons Exploration (MMX). Earth, Planets and Space 73; 1-14. https://doi.org/10.1186/s40623-021-01462-9

Kaplan HH, Lauretta DS, Simon AA, Hamilton VE, DellaGiustina DN, Golish DR, Reuter DC, Bennett CA, Burke KN, Campins H, Connolly Jr HC, Dworkin JP, Emery JP, Glavin DP, Glitch TD, Hanna R, Ishimaru K, Jawin ER, McCoy TJ, Porter N, Sandford SA, Ferrone S, Clark BE, Li J-Y, Zou X-D, Daly MG, Barnouin OS, Seabrook JA, Enos HL (2020) Bright carbonate veins on asteroid (101955) Bennu:Implications for aqueous alteration history. Science 370:abc3557. https://doi.org/10.1126/science.abc3557

Kawaguchi JI., Fujiwara A, Uesugi T (2008) Hayabusa—Its technology and science accomplishment summary and Hayabusa-2. Acta Astronautica 62:639-647. https://doi.org/10.1016/j.actaastro.2008.01.028

Kebukawa, Y., Quirico, E., Dartois, E., Yabuta, H., Bejach, L., Bonal, L., Dazzi, A., Deniset-Besseau, A., Duprat, J., Engrand, C., Mathurin, J., Barosch, J., Cody, G.D., De Gregorio, B., Hashiguchi, M., Kamide, K., Kilcoyne, D., Komatsu, M., Martins, Z., Montagnac, G., Mostefaoui, S., Nittler, L.R., Ohigashi, T., Okumura, T., Remusat, L., Sandford, S., Shigenaka, M., Stroud, R., Suga, H., Takahashi, Y., Takeichi, Y.,

Tamenori, Y., Verdier-Paoletti, M., Wakabayashi, D., Yamashita, S., Yurimoto, H., Nakamura, T., Noguchi, T., Okazaki, R., Naraoka, H., Sakamoto, K., Tachibana, S., Yada, T., Nishimura, M., Nakato, A., Miyazaki, A., Yogata, K., Abe, M., Okada, T., Usui, T., Yoshikawa, M., Saiki, T., Tanaka, S., Terui, F., Nakazawa, S., Watanabe, S., Tsuda, Y. (2024). Infrared absorption spectra from organic matter in the asteroid Ryugu samples: Some unique properties compared to unheated carbonaceous chondrites. Meteoritics & Planetary Science 59, 1845–1858. https://doi.org/10.1111/maps.14064

Keller LP, Berger EL (2014) A transmission electron microscope study of Itokawa regolith grains. Earth, Planets and Space 66:1-7. https://doi.org/10.1186/1880-5981-66-71

Kikuchi S, Saiki T, Takei Y et al (2021) Hayabusa2 pinpoint touchdown near the artificial crater on Ryugu: Trajectory design and guidance performance. Advances in Space Research 68:3093-3140. https://doi.org/10.1016/j.asr.2021.07.031

Kikuchi S, Watanabe SI, Saiki T et al (2020) Hayabusa2 landing site selection: surface topography of Ryugu and touchdown safety. Space Science Reviews 216:1-67. https://doi.org/10.1007/s11214-020-00737-z

Kitazato K, Milliken RE, Iwata T et al (2019) The surface composition of asteroid 162173 Ryugu from Hayabusa2 near-infrared spectroscopy. Science 364:272-275. https://doi.org/10.1126/science.aav7432

Kuninaka H, Nishiyama K, Funaki I et al (2007) Powered flight of electron cyclotron resonance ion engines on Hayabusa explorer. Journal of Propulsion and Power 23:544-551. https://doi.org/10.2514/1.25434

Kuramoto K, Kawakatsu Y, Fujimoto M et al (2022) Martian moons exploration MMX: sample return mission to Phobos elucidating formation processes of habitable planets. Earth, Planets and Space, 74:12. https://doi.org/10.1186/s40623-021-01545-7

Lantz C, Brunetto R, Barucci MA et al (2017). Ion irradiation of carbonaceous chondrites: A new view of space weathering on primitive asteroids. Icarus 285:43-57. https://doi.org/10.1016/j.icarus.2016.12.019

Lauretta, D. S., and Connolly, Harold C., Aebersold, Joseph E., Alexander, Conel M. O'D., Ballouz, Ronald-L., Barnes, Jessica J., Bates, Helena C., Bennett, Carina A., Blanche, Laurinne, Blumenfeld, Erika H., Clemett, Simon J., Cody, George D., DellaGiustina, Daniella N., Dworkin, Jason P., Eckley, Scott A., Foustoukos, Dionysis I., Franchi, Ian A., Glavin, Daniel P., Greenwood, Richard C., Haenecour, Pierre, Hamilton, Victoria E., Hill, Dolores H., Hiroi, Takahiro, Ishimaru, Kana, Jourdan, Fred, Kaplan, Hannah H., Keller, Lindsay P., King, Ashley J., Koefoed, Piers, Kontogiannis, Melissa K., Le, Loan, Macke, Robert J., McCoy, Timothy J., Milliken, Ralph E., Najorka, Jens, Nguyen, Ann N., Pajola, Maurizio, Polit, Anjani T., Righter, Kevin, Roper, Heather L., Russell, Sara S., Ryan,,rew J., Sandford, Scott A., Schofield, Paul F., Schultz, Cody D., Seifert, Laura B., Tachibana, Shogo, Thomas-Keprta, Kathie L., Thompson, Michelle S., Tu, Valerie, Tusberti, Filippo, Wang, Kun,

Zega, Thomas J., Wolner, C. W. V., Team, the OSIRIS-REx Sample Analysis (2024). "Asteroid (101955) Bennu in the laboratory: Properties of the sample collected by OSIRIS-REx." Meteoritics and Planetary Science: 1-34.

Lauretta DS, Adam CD, Allen AJ et al (2022) Spacecraft sample collection and subsurface excavation of asteroid (101955) Bennu. Science 377:285-291. https://doi.org/10.1126/science.abm1018

Lauretta DS, Bartels AE, Barucci MA (2015) The OSIRIS-REx target asteroid (101955) Bennu: Constraints on its physical, geological, and dynamical nature from astronomical observations. Meteoritics & Planetary Science 50:834-849. https://doi.org/10.1111/maps.12353

Lauretta DS, DellaGiustina DN, Bennett CA et al (2019) The unexpected surface of asteroid (101955) Bennu. Nature 568:55-60. https://www.nature.com/articles/s41586-019-1033-6

Lauretta DS and Hergenrother CW et al. (2019) Episodes of particle ejection from the surface of the active asteroid (101955) Bennu. Science 366 eaay3544.. https://doi.org/10.1126/science.aay3544

Lauretta DS, Connolly Jr HCC, Grossman JN, Polit AT, the OSIRIS-REx Sample analysis team (2023) OSIRIS-REx Sample Analysis Plan – Revision 3.0. arXiv:2308.11794. https://doi.org/10.48550/arXiv.2308.11794

Lawrence DJ, Peplowski PN, Beck AW et al (2019) Measuring the Elemental Composition of Phobos: The Mars-moon Exploration with GAmma rays and NEutrons (MEGANE) Investigation for the Martian Moons eXploration (MMX) Mission. Earth and Space Science 6; 2605-2623. https://doi.org/10.1029/2019EA000811.

LeCorre L, Reddy V, Bottke WF, DellaGiustina DN, Burke KN, Molau J, Van Auken RB, Golish DR, Sanchez JA, Li J-Y, d'Aubigny CYD, Rizk B, Lauretta DS (2021) Characterization of exogenic boulders on near-Earth asteroid (101955) Bennu from OSIRIS-REx color images. The Planetary Science Journal 2:114. https://doi.org/10.3847/PSJ/abfbe2

Liu MC, McCain KA, Matsuda N et al (2022) Incorporation of 16O-rich anhydrous silicates in the protolith of highly hydrated asteroid Ryugu. Nat Astron 6:1172–1177. https://doi.org/10.1038/s41550-022-01762-4

Loizeau D, Pilorget C, Riu L et al (2023) Constraints on Solar System early evolution by MicrOmega analysis of Ryugu carbonates. Nature Astronomy 7:391-397. https://www.nature.com/articles/s41550-022-01870-1

Ma C, Nakamura T, Mikouchi T et al (2022) Mg-Phosphate from Asteroid Ryugu: An Original H2O-Rich Phase. LPI Contributions 2695:6134.

Marrocchi Y, Piralla M, Tissot FL (2023) Iron Isotope Constraints on the Structure of the Early Solar System. The Astrophysical Journal Letters 954:L27. https://doi.org/10.3847/2041-8213/acefd1

Masterson, R.A., Chodas, M., Bayley, L., Allen, B., Hong, J., Biswas, P., McMenamin,

C., Stout, K., Bokhour, E., Bralower, H., Carte, D., Chen, S., Jones, M., Kissel, S., Schmidt, F., Smith., M., Sondecker, G., Lim, L.F., Lauretta, D.S., Grindlay, J.E., Binzel, R.P. (2018) Regolith X-Ray Imaging Spectrometer (REXIS) Aboard the OSIRIS-REx Asteroid Sample Return Mission. Space Sci Rev 214:48. https://doi.org/10.1007/s11214-018-0483-8

Mathurin, J., Bejach, L., Dartois, E., Engrand, C., Dazzi, A., Deniset-Besseau, A., Duprat, J., Kebukawa, Y., Yabuta, H., Bonal, L., Quirico, E., Sandt, C., Borondics, F., Barosch, J., Beck, P., Cody, G.D., Gregorio, B.T.D., Hashiguchi, M., Kilcoyne, D.A.L., Komatsu, M., Martins, Z., Matsumoto, M., Montagnac, G., Mostefaoui, S., Nittler, L.R., Ohigashi, T., Okumura, T., Phan, V.T.H., Remusat, L., Sandford, S., Shigenaka, M., Stroud, R., Suga, H., Takahashi, Y., Takeichi, Y., Tamenori, Y., Verdier-Paoletti, M., Yamashita, S., Nakamura, T., Morita, T., Kikuiri, M., Amano, K., Kagawa, E., Noguchi, T., Naraoka, H., Okazaki, R., Sakamoto, K., Yurimoto, H., Abe, M., Kamide, K., Miyazaki, A., Nakato, A., Nakazawa, S., Nishimura, M., Okada, T., Saiki, T., Tachibana, S., Tanaka, S., Terui, F., Tsuda, Y., Usui, T., Watanabe, S., Yada, T., Yogata, K., Yoshikawa, M. (2024) AFM-IR nanospectroscopy of nanoglobule-like particles in Ryugu samples returned by the Hayabusa2 mission. Astronomy & Astrophysics 684, A198. https://doi.org/10.1051/0004-6361/202347435

Matsumoto T, Hasegawa S, Nakao S et al (2018) Population characteristics of submicrometer-sized craters on regolith particles from asteroid Itokawa. Icarus 303:22-33. https://doi.org/10.1016/j.icarus.2017.12.017

Matsumoto M, Matsuno J, Tsuchiyama A et al (2024) Microstructural and chemical features of impact melts on Ryugu particle surfaces: Records of interplanetary dust hit on asteroid Ryugu. Science Advances 10:eadi7203. https://doi.org/10.1126/sciadv.adi7203

Matsumoto T, Harries D, Langenhorst F et al (2020) Iron whiskers on asteroid Itokawa indicate sulfide destruction by space weathering. Nature communications 11:1117. https://www.nature.com/articles/s41467-020-14758-3

Matsuoka M, Kagawa EI, Amano K et al (2023) Space weathering acts strongly on the uppermost surface of Ryugu. Communications Earth & Environment 4:335. https://www.nature.com/articles/s43247-023-00991-3

McCain KA, Matsuda N, Liu MC et al (2023) Early fluid activity on Ryugu inferred by isotopic analyses of carbonates and magnetite. Nature Astronomy 7:309-317. https://www.nature.com/articles/s41550-022-01863-0

McCoy, T. J., and Russell, S. S., Zega, T. J., Thomas-Keprta, K. L., Singerling, S. A., Brenker, F. E., Timms, N. E., Rickard, W. D. A., Barnes, J. J., Libourel, G., Ray, S., Corrigan, C. M., Haenecour, P., Gainsforth, Z., Dominguez, G., King, A. J., Keller, L. P., Thompson, M. S., Sandford, S. A., Jones, R. H., Yurimoto, H., Righter, K., Eckley, S. A., Bland, P. A., Marcus, M. A., DellaGiustina, D. N., Ireland, T. R., Almeida, N. V., Harrison, C. S., Bates, H. C., Schofield, P. F., Seifert, L. B., Sakamoto, N., Kawasaki, N., Jourdan, F., Reddy, S. M., Saxey, D. W., Ong, I. J., Prince, B. S.,

Ishimaru, K., Smith, L. R., Benner, M. C., Kerrison, N. A., Portail, M., Guigoz, V., Zanetta, P.-M., Wardell, L. R., Gooding, T., Rose, T. R., Salge, T., Le, L., Tu, V. M., Zeszut, Z., Mayers, C., Sun, X., Hill, D. H., Lunning, N. G., Hamilton, V. E., Glavin, D. P., Dworkin, J. P., Kaplan, H. H., Franchi, I. A., Tait, K. T., Tachibana, S., Connolly, H. C., Lauretta, D. S. (2025) An evaporite sequence from ancient brine recorded in Bennu samples. Nature 637:1072-1077. https://doi.org/10.1038/s41586-024-08495-6

Michel P, Richardson DC (2013) Collision and gravitational reaccumulation: Possible formation mechanism of the asteroid Itokawa. Astronomy & Astrophysics 554:L1. https://doi.org/10.1051/0004-6361/201321657

Michikami T, Honda C, Miyamoto H et al (2019) Boulder size and shape distributions on asteroid Ryugu. Icarus 331:179-191. https://doi.org/10.1016/j.icarus.2019.05.019

Mikouchi T., Yoshida H., Hayashi S., Masuda M., Sugiyama K., Nakamura T., Zolensky M. (2024) Amorphous magnesium phosphate in asteroid Ryugu samples and CI chondrites. *87th Meeting of The Meteoritical Society.* Abstract.

Miyamoto H, Yano H, Scheeres DJ et al (2007) Regolith migration and sorting on asteroid Itokawa. Science 316:1011-1014. https://doi.org/10.1126/science.1134390

Morota T, Sugita S, Cho Y et al (2020) Sample collection from asteroid (162173) Ryugu by Hayabusa2: Implications for surface evolution. Science 368:654-659. https://doi.org/10.1126/science.aaz6306

Muirhead BK, Nicholas A, Umland J (2020) Mars sample return mission concept status. In 2020 IEEE Aerospace Conference:1-8. IEEE. https://doi.org/10.1109/AERO47225.2020.9172609.

Nagao K, Okazaki R, Nakamura T et al (2011) Irradiation history of Itokawa regolith material deduced from noble gases in the Hayabusa samples. Science 333:1128-1131. https://doi.org/10.1126/science.1207785

Nakamura AM, Michikami T, Hirata N et al (2008) Impact process of boulders on the surface of asteroid 25143 Itokawa—fragments from collisional disruption. Earth Planet Sp 60:7-12. https://doi.org/10.1186/BF03352756

Nakamura E, Kobayashi K, Tanaka R et al (2022) On the origin and evolution of the asteroid Ryugu: A comprehensive geochemical perspective. Proceedings of the Japan Academy, Series B 98:227-282. https://doi.org/10.2183/pjab.98.015

Nakamura T, Nakato A, Ishida H et al (2014) Mineral chemistry of MUSES-C Regio inferred from analysis of dust particles collected from the first-and second-touchdown sites on asteroid Itokawa. Meteoritics & Planetary Science 49:215-227. https://doi.org/10.1111/maps.12247

Nakamura T, Noguchi T, Tsuchiyama A et al (2008) Chondrulelike objects in short-period comet 81P/Wild 2. Science 321:1664-1667.

https://doi.org/10.1126/science.1160995

Nakamura T, Noguchi T, Tanaka M et al (2011) Itokawa dust particles: a direct link between S-type asteroids and ordinary chondrites. Science 333:1113-1116. https://doi.org/10.1126/science.1207758

Nakamura T, Ikeda H, Kouyama T et al (2021) Science operation plan of Phobos and Deimos from the MMX spacecraft. Earth, Planets and Space 73:227. https://doi.org/10.1186/s40623-021-01546-6

Nakamura T, Matsumoto M, Amano K et al (2022) Formation and evolution of carbonaceous asteroid Ryugu: Direct evidence from returned samples. Science 379:eabn8671. https://doi.org/10.1126/science.abn8671

Nakashima D, Nakamura T, Zhang M et al (2023) Chondrule-like objects and Ca-Al-rich inclusions in Ryugu may potentially be the oldest Solar System materials. Nature communications 14:532. https://www.nature.com/articles/s41467-023-36268-8

Naraoka H, Takano Y, Dworkin JP et al (2023) Soluble organic molecules in samples of the carbonaceous asteroid (162173) Ryugu. Science 379:eabn9033. https://doi.org/10.1126/science.abn9033

Nguyen AN, Mane P, Keller LP et al (2023) Abundant presolar grains and primordial organics preserved in carbon-rich exogenous clasts in asteroid Ryugu. Science advances 9:eadh1003. https://doi.org/10.1126/sciadv.adh1003

Ninomiya K, Osawa T, Terada K et al (2023) Quantification of bulk elemental composition for C-type asteroid Ryugu samples with nondestructive elemental analysis using muon beam. Meteoritics & Planetary Science in press. https://doi.org/10.1111/maps.14135

Nishiyama G, Kawamura T, Namiki N et al (2021). Simulation of seismic wave propagation on asteroid ryugu induced by the impact experiment of the hayabusa2 mission: Limited mass transport by low yield strength of porous regolith. Journal of Geophysical Research: Planets 126:e2020JE006594. https://doi.org/10.1029/2020JE006594

Noguchi T, Kimura M, Hashimoto T et al (2014a) Space weathered rims found on the surfaces of the Itokawa dust particles. Meteoritics & Planetary Science 49:188-214. https://doi.org/10.1111/maps.12111

Noguchi T, Kimura M, Hashimoto T et al (2014b) Sylvite and halite on particles recovered from 25143 Itokawa: A preliminary report. Meteoritics & Planetary Science 49:1305-1314. https://doi.org/10.1111/maps.12333

Noguchi T, Matsumoto T, Miyake A et al (2023a) A dehydrated space-weathered skin cloaking the hydrated interior of Ryugu. Nature Astronomy 7:170-181. https://www.nature.com/articles/s41550-022-01841-6

Noguchi T, Nakamura T, Kimura M et al (2011) Incipient space weathering observed

on the surface of Itokawa dust particles. Science 333:1121-1125. https://doi.org/10.1126/science.1207794

Noguchi T, Tsuchiyama A, Hirata N et al (2010) Surface morphological features of boulders on Asteroid 25143 Itokawa. Icarus 206:319-326. https://doi.org/10.1016/j.icarus.2009.09.002

Okada T, Fukuhara T, Tanaka S (2020) Highly porous nature of a primitive asteroid revealed by thermal imaging. Nature 579:518-522. https://www.nature.com/articles/s41586-020-2102-6

Okazaki R, Yamanouchi S, Shimada K et al (2022) Methods and tools for handling, transportation, weighing, and pelletization applied to the initial analysis of volatile components in the Hayabusa2 samples, Earth, Planets and Space 74: 190. https://doi.org/10.1186/s40623-022-01747-7

Okazaki R, Marty B, Busemann H et al (2022). Noble gases and nitrogen in samples of asteroid Ryugu record its volatile sources and recent surface evolution. Science 379:eabo0431. https://doi.org/10.1126/science.abo0431

Okazaki R, Miura YN, Takano Y et al (2022) First asteroid gas sample delivered by the Hayabusa2 mission: A treasure box from Ryugu. Science advances 8:eabo7239. https://doi.org/10.1126/sciadv.abo7239

Osawa T, Nagasawa S, Ninomiya K et al (2023) Development of Nondestructive Elemental Analysis System for Hayabusa2 Samples Using Muonic X-rays. ACS Earth and Space Chemistry 7:699-711. https://doi.org/10.1021/acsearthspacechem.2c00303

Ostro SJ, Benner LA, Nolan MC et al (2004) Radar observations of asteroid 25143 Itokawa (1998) Meteoritics & Planetary Science 39:407-424. https://doi.org/10.1111/j.1945-5100.2004.tb00102.x

Park J, Turrin BD, Herzog GF et al (2015) 40Ar/39Ar age of material returned from asteroid 25143 Itokawa. Meteoritics & Planetary Science 50:2087-2098. https://doi.org/10.1111/maps.12564

Parker, E.T., Chan, Q.H.S., Glavin, D.P., Dworkin, J.P. (2022) Non-protein amino acids identified in carbon-rich Hayabusa particles. Meteoritics & Planetary Science 57: 776–793. https://doi.org/10.1111/maps.13794

Parker, E.T., McLain, H.L., Glavin, D.P., Dworkin, J.P., Elsila, J.E., Aponte, J.C., Naraoka, H., Takano, Y., Tachibana, S., Yabuta, H., Yurimoto, H., Sakamoto, K., Yada, T., Nishimura, M., Nakato, A., Miyazaki, A., Yogata, K., Abe, M., Okada, T., Usui, T., Yoshikawa, M., Saiki, T., Tanaka, S., Nakazawa, S., Tsuda, Y., Terui, F., Noguchi, T., Okazaki, R., Watanabe, S., Nakamura, T. (2023) Extraterrestrial amino acids and amines identified in asteroid Ryugu samples returned by the Hayabusa2 mission. Geochimica et Cosmochimica Acta 347: 42–57. https://doi.org/10.1016/j.gca.2023.02.017

Paquet M, Moynier F, Yokoyama T et al (2023) Contribution of Ryugu-like material to Earth's volatile inventory by Cu and Zn isotopic analysis. Nature astronomy 7:182-189. https://www.nature.com/articles/s41550-022-01846-1

Phan, V.T.H., Beck, P., Rebois, R., Quirico, E., Noguchi, T., Matsumoto, T., Miyake, A., Igami, Y., Haruta, M., Saito, H., Hata, S., Seto, Y., Miyahara, M., Tomioka, N., Ishii, H.A., Bradley, J.P., Ohtaki, K.K., Dobricǎ, E., Leroux, H., Le Guillou, C., Jacob, D., de la Peña, F., Laforet, S., Marinova, M., Langenhorst, F., Harries, D., Abreu, N.M., Gray, J., Zega, T., Zanetta, P.-M., Thompson, M.S., Stroud, R., Mathurin, J., Dazzi, A., Dartois, E., Engrand, C., Burgess, K., Cymes, B.A., Bridges, J.C., Hicks, L., Lee, M.R., Daly, L., Bland, P.A., Zolensky, M.E., Frank, D.R., Martinez, J., Tsuchiyama, A., Yasutake, M., Matsuno, J., Okumura, S., Mitsukawa, I., Uesugi, K., Uesugi, M., Takeuchi, A., Sun, M., Enju, S., Takigawa, A., Michikami, T., Nakamura, T., Matsumoto, M., Nakauchi, Y., Abe, M., Nakazawa, S., Okada, T., Saiki, T., Tanaka, S., Terui, F., Yoshikawa, M., Miyazaki, A., Nakato, A., Nishimura, M., Usui, T., Yada, T., Yurimoto, H., Nagashima, K., Kawasaki, N., Sakamotoa, N., Hoppe, P., Okazaki, R., Yabuta, H., Naraoka, H., Sakamoto, K., Tachibana, S., Watanabe, S., Tsuda, Y. (2024) In situ investigation of an organic micro-globule and its mineralogical context within a Ryugu "sand" grain. Meteoritics & Planetary Science, in press. https://doi.org/10.1111/maps.14122

Pignatale F C, Charnoz S, Rosenblatt P. et al (2018) On the impact origin of Phobos and Deimos. III. Resulting composition from different impactors. The Astrophysical Journal 853; 118. https://doi.org/10.3847/1538-4357/aaa23e

Pilorget C, Okada T, Hamm V et al (2022) First compositional analysis of Ryugu samples by the MicrOmega hyperspectral microscope. Nature Astronomy 6:221-225. https://www.nature.com/articles/s41550-021-01549-Z

Pilorget C et al (2024) Phosphorus-rich grains in Ryugu samples with major biochemical potential. Nature Astronomy: 1-7.

Pinilla-Alonso N, de León J, Walsh KJ et al (2016) Portrait of the Polana-Eulalia family complex: surface homogeneity revealed from near-infrared spectroscopy. Icarus 274:231-248. https://doi.org/10.1016/j.icarus.2016.03.022

Potiszil, C., Ota, T., Yamanaka, M., Sakaguchi, C., Kobayashi, K., Tanaka, R., Kunihiro, T., Kitagawa, H., Abe, M., Miyazaki, A., Nakato, A., Nakazawa, S., Nishimura, M., Okada, T., Saiki, T., Tanaka, S., Terui, F., Tsuda, Y., Usui, T., Watanabe, S., Yada, T., Yogata, K., Yoshikawa, M., Nakamura, E. (2023) Insights into the formation and evolution of extraterrestrial amino acids from the asteroid Ryugu. Nature Communications 14: 1482. https://doi.org/10.1038/s41467-023-37107-6

Praet A, Barucci MA, Clark BE, Kaplan HH, Simon AA, Hamilton VE, Emery JP, Howell ES, Lim LF, Zou X-D, Li J-Y, Reuter DC, Merlin F, Deshapriya JDP,

Fornasier A, Hasselmann PH, Poggiali G, Ferrone S, Brucato JR, Takir D, Cloutis E, Connolly, Jr HC, Fulchignoni M, Lauretta DS (2021) Hydrogen abundance estimation and distribution on (101955) Bennu. Icarus 363:114427. https://doi.org/10.1016/j.icarus.2021.114427

Quirico, E., Bonal, L., Kebukawa, Y., Amano, K., Yabuta, H., Phan, V.T.H., Beck, P., Rémusat, L., Dartois, E., Engrand, C., Martins, Z., Bejach, L., Dazzi, A., Deniset-Besseau, A., Duprat, J., Mathurin, J., Montagnac, G., Barosch, J., Cody, G.D., De Gregorio, B., Enokido, Y., Hashiguchi, M., Kamide, K., Kilcoyne, D., Komatsu, M., Matsumoto, M., Mostefaoui, S., Nittler, L., Ohigashi, T., Okumura, T., Sandford, S., Shigenaka, M., Stroud, R., Suga, H., Takahashi, Y., Takeichi, Y., Tamenori, Y., Verdier-Paoletti, M., Wakabayashi, D., Yamashita, S., Nakamura, T., Naraoka, H., Noguchi, T., Okazaki, R., Yurimoto, H., Sakamoto, K., Tachibana, S., Watanabe, S.-I., Tsuda, Y., Yada, T., Nishimura, M., Nakato, A., Miyazaki, A., Yogata, K., Abe, M., Okada, T., Usui, T., Yoshikawa, M., Saiki, T., Tanaka, S., Terui, F., Nakazawa, S. (2024) Compositional heterogeneity of insoluble organic matter extracted from asteroid Ryugu samples. Meteoritics & Planetary Science, in press. https://doi.org/10.1111/maps.14097

Reuter DC, Simon AA, Hair J, Lunsford A, Manthripragada S, Bly V, Bos B, Brambora C, Caldwell E, Casto G, Dolch Z, Finneran P, Jennings D, Jhabvala M, Matson E, McLelland M, Roher W, Sullivan T, Weigle E, Wen Y, Wilson, D, Lauretta DS (2018). The OSIRIS-REx Visible and InfraRed Spectrometer (OVIRS): Spectral Maps of the Asteroid Bennu. Space Science Reviews 214:1–22.

Riu L, Pilorget C, Milliken R et al (2021) Spectral characterization of the craters of Ryugu as observed by the NIRS3 instrument on-board Hayabusa2. Icarus 357:114253. https://doi.org/10.1016/j.icarus.2020.114253

Rivkin AS, Brown RH, Trilling DE et al (2002) Near-infrared spectrophotometry of Phobos and Deimos. Icarus 156; 64-75. https://doi.org/10.1006/icar.2001.6767

Rizk, B., d'Aubigny, C. D., Golish, D., Fellows, C., Merrill, C., Smith, P., Walker, M.S., Hendershot, J.E., Hancock, J., Bailey, S. H., DellaGiustina, D. N., Lauretta, D.S., Tanner, R., Williams, M., Harshman, K., Fitzgibbon, M., Verts, W., Chen, J., Connors, T., Hamara, D., Dowd, A., Lowman, A., Dubin, M., Burt, R., Whiteley, M., Watson, M., McMahon, T., Ward, M., Booher, D., Read, M., Williams, B., Hunten, M., Little, E., Saltzman, T., Alfred, D., O'Dougherty, S., Walthall, M., Kenagy, K., Peterson, S., Crowther, B., Perry, M.L., See, C., Selznick, S., Suave, C., Beiser, M., Black, W, Pfisterer, R.N., Lancaster, A., Oliver, S., Oquest, C., Crowley, D., Morgan, C., Castle, C., Dominguez, R., Sullivan, M. (2018). OCAMS: the OSIRIS-REx camera suite. Space Sci Rev, 214(1), 26.

Rosenblatt P, Charnoz S, Dunseath KM et al (2016) Accretion of Phobos and Deimos in an extended debris disc stirred by transient moons. Nature Geoscience 9; 581-583. https://doi.org/10.1038/ngeo2742

Rozitis B, Emery JP, Siegler MA, Susorney HCM, Molaro JL, Hergnrother CW, Lauretta DS (2020) Implications for ice stability and particle ejection from high-

resolution temperature modeling of asteroid (101955) Bennu. Journal of Geophysical Research - Planets 125:e2019JE006323. https://doi.org/10.1029/2019JE006323

Rubin AE, Trigo-Rodriguez JM, Huber H, Wasson JT (2007) Progressive aqueous alteration of CM carbonaceous chondrites. Geochimica et Cosmochimica Acta 71:2361-2382. https://doi.org/10.1016/j.gca.2007.02.008

Rubincam DP (2000) Radiative spin-up and spin-down of small asteroids. Icarus 148:2-11. https://doi.org/10.1006/icar.2000.6485

Ryan, A. J., R.-L. Ballouz, R. J. Macke, H. C. Connolly and D. S. Lauretta (2024). Physical and thermal properties of OSIRIS-REx Samples: Insight into the evolution of Bennu and its Regolith. Lunar and Planetary Science **LV**: 1594.

Saito J, Miyamoto H, Nakamura R et al (2006) Detailed images of asteroid 25143 Itokawa from Hayabusa. Science 312:1341-1344. https://doi.org/10.1126/science.1125722

Sawada H, Okazaki R, Tachibana S et al (2017). Hayabusa2 sampler: collection of asteroidal surface material. Space Science Reviews 208:81-106. https://doi.org/10.1007/s11214-017-0338-8

Scheeres DJ, McMahon JW, French AS, Brack DN, Chesley SR, Farnocchia D, Takahashi Y, Leonard JM, Geeraert J, Page P, Antreasian P, Getzandanner K, Rowlands D, Mazarico EM, Small J, Highsmith DE, Moreau M, Emery JP, Rozitis B, Hirabayashi M, Sánchez P, Van wal S, Tricarico P, Ballouz R-L, Johnson CL, Al Asad MM, Susorney HCM, Barnouin OS, Daly MG, Seabrook JA, Gaskell RW, Palmer EE, Weirich JR, Walsh KJ, Jawin ER, Bierhaus EB, Michel P, Bottke WF, Nolan MC, Connolly,Jr HC, Lauretta DS and the OSIRIS-REx Team (2019). The dynamic geophysical environment of (101955) Bennu based on OSIRIS-REx measurements. Nature Astronomy 3:352–361. https://doi.org/10.1038/s41550-019-0721-3

Scheeres DJ, Abe M, Yoshikawa M et al (2007) The effect of YORP on Itokawa. Icarus 188:425-429. https://doi.org/10.1016/j.icarus.2006.12.014

Scheeres DJ, Hesar SG, Tardivel S, Hirabayashi M, Farnocchia D, McMahon JW, Chesley SR, Barnouin O, Binzel RP, Bottle WR, Daly MG, Emery JP, Hergnrother CW, Lauretta DS, Marshall JR, Michel P, Nolan MC, Walsh KJ (2016) The geophysical environment of Bennu. Icarus 276:116-140. https://doi.org/10.1016/j.icarus.2016.04.013

Schmitt-Kopplin, P., Hertkorn, N., Harir, M., Moritz, F., Lucio, M., Bonal, L., Quirico, E., Takano, Y., Dworkin, J.P., Naraoka, H., Tachibana, S., Nakamura, T., Noguchi, T., Okazaki, R., Yabuta, H., Yurimoto, H., Sakamoto, K., Yada, T., Nishimura, M.,

Nakato, A., Miyazaki, A., Yogata, K., Abe, M., Usui, T., Yoshikawa, M., Saiki, T., Tanaka, S., Terui, F., Nakazawa, S., Okada, T., Watanabe, S., Tsuda, Y., Hayabusa2-initial-analysis SOM team, H.S. team, Hayabusa2-initial-analysis SOM team, Hayabusa2-initial-analysis SOM team, Hayabusa2-initial-analysis SOM team, Hayabusa2-initial-analysis SOM team, Hamase, Kenji, Furusho, A., Hashiguchi, M., Fukushima, K., Aoki, D., Aponte, J.C., Parker, E.T., Glavin, D.P., McLain, H.L., Elsila, J.E., Graham, H.V., Eiler, J.M., Ruf, A., Orthous-Daunay, F.-R., Isa, J., Vuitton, V., Thissen, R., Ogawa, N.O., Sakai, S., Yoshimura, T., Koga, T., Sugahara, H., Ohkouchi, N., Mita, H., Furukawa, Y., Oba, Y., Oba, Y. (2023). Soluble organic matter Molecular atlas of Ryugu reveals cold hydrothermalism on C-type asteroid parent body. Nature Communications 14: 6525. https://doi.org/10.1038/s41467-023-42075-y

Shimaki Y, Senshu H, Sakatani N et al (2020) Thermophysical properties of the surface of asteroid 162173 Ryugu: Infrared observations and thermal inertia mapping. Icarus 348:113835. https://doi.org/10.1016/j.icarus.2020.113835

Simon AA, Kaplan HH, Hamilton VE et al (2020) Widespread carbon-bearing materials on near-Earth asteroid (101955) Bennu. Science 370:eabc3522. https://doi.org/10.1126/science.abc3522

Stöffler D, Keil K (1991) Shock metamorphism of ordinary chondrites. Geochimica et Cosmochimica Acta 55:3845-3867. https://doi.org/10.1016/0016-7037(91)90078-J

Sugita S, Honda R, Morota T et al (2019) The geomorphology, color, and thermal properties of Ryugu: Implications for parent-body processes. Science 364:eaaw0422. https://doi.org/10.1126/science.aaw0422

Tachibana S, Sawada H, Okazaki R et al (2022) Pebbles and sand on asteroid (162173) Ryugu: In situ observation and particles returned to Earth. Science 375:1011-1016. https://doi.org/10.1126/science.abj8624

Takir D, Emery JP, McSween Jr. HY, Hibbitts CA, Clark RN, Pearson N, Wang A. (2013) Nature and degree of aqueous alteration in CM and CI carbonaceous chondrites. Meteoritics & Planetary Science 48:1618-1637. https://doi: 10.1111/maps.12171

Tatsumi E, Domingue D, Schröder S et al (2020) Global photometric properties of (162173) Ryugu. Astronomy & Astrophysics 639:A83. https://doi.org/10.1051/0004-6361/201937096

Terada K, Sano Y, Takahata N et al (2018) Thermal and impact histories of 25143 Itokawa recorded in Hayabusa particles. Scientific reports 8:11806. https://doi.org/10.1038/s41598-018-30192-4

Tholen, DJ (1989) Asteroid taxonomic classifications. In Asteroids II (R. P. Binzel et al. eds.), pp. 1139–1150. Univ. of Arizona, Tucson.

Thompson MS, Christoffersen R, Zega TJ et al (2014) Microchemical and structural

evidence for space weathering in soils from asteroid Itokawa. Earth Planet Sp 66:89. https://doi.org/10.1186/1880-5981-66-89

Thompson MS, Loeffler MG, Morris RV, Keller LP, Christoffersen R (2019) Spectral and chemical effects of simulated space weathering of the Murchison CM2 carbonaceous chondrite. Icarus 319:499-511. https://10.1016/j.icarus.2018.09.022

Tsuchiyama A, Uesugi M, Matsushima T et al (2011) Three-dimensional structure of Hayabusa samples: origin and evolution of Itokawa regolith. science 333:1125-1128. https://doi.org/10.1126/science.1207807

Tsuda Y, Saiki T, Terui F et al (2020) Hayabusa2 mission status: Landing, roving and cratering on asteroid Ryugu. Acta Astronautica 171:42-54. https://doi.org/10.1016/j.actaastro.2020.02.035

Tsuda Y, Yoshikawa M, Abe M et al (2013) System design of the Hayabusa 2—Asteroid sample return mission to 1999 JU3. Acta Astronautica 91:356-362. https://doi.org/10.1016/j.actaastro.2013.06.028

Van Schmus WR and Wood JA (1967) A chemical-petrologic classification for the chondritic meteorites. Geochimica et Cosmochimica Acta 31:747-765.

Veverka J, Klaasen K, A'Hearn M et al (2013) Return to comet Tempel 1: overview of Stardust-NExT results. Icarus 222:424-435. https://doi.org/10.1016/j.icarus.2012.03.034

Viennet, J.C., Roskosz, M., Nakamura, T., Beck, P., Baptiste, B., Lavina, B., Alp, E.E., Hu, M.Y., Zhao, J., Gounelle, M., Brunetto, R., Yurimoto, H., Noguchi, T., Okazaki, R., Yabuta, H., Naraoka, H., Sakamoto, K., Tachibana, S., Yada, T., Nishimura, M., Nakato, A., Miyazaki, A., Yogata, K., Abe, M., Okada, T., Usui, T., Yoshikawa, M., Saiki, T., Tanaka, S., Terui, F., Nakazawa, S., Watanabe, S.I., Tsuda, Y (2023) Interaction between clay minerals and organics in asteroid Ryugu. Geochemical Perspectives Letters 25, 8–12. https://doi.org/10.7185/geochemlet.2307

Vilas F, Gaffey MJ (1989) Phyllosilicate absorption features in main-belt and outer-belt asteroid reflectance spectra. Science 246:790-792. https://doi.org/10.1126/science.246.4931.790

Wakita S, Nakamura T, Ikeda T et al (2014) Thermal modeling for a parent body of Itokawa. Meteoritics & Planetary Science 49:228-236. https://doi.org/10.1111/maps.12174

Walsh KJ (2018) Rubble pile asteroids. Annual Review of Astronomy and Astrophysics 56:593-624. https://doi.org/10.1146/annurev-astro-081817-052013

Walsh KJ, Jawin ER, Ballouz R-L, Barnouin OS, Bierhaus EB, Connolly, Jr HC, Molaro JL, McCoy TJ, Delbo M, Hartzell CM, Pajola M, Schwartz SR, Trang D, Asphaug E, Becker KJ, Beddingfield CB, Bennett CA, Bottke WF, Burke KN, Clark

BC, Daly MG, DellaGiustina DN, Dworkin JP, Elder CM, Golish DR, Hildebrand AR, Malhotra R, Marshall J, Michel P, Nolan MC, Perry ME, Rizk B, Ryan A, Sandford SA, Scheeres DJ, Susorney HCM, Thuillet F, Lauretta DS, the OSIRIS-REx Team (2019) Craters, boulders and regolith of (101955) Bennu indicative of an old and dyn amic surface. Nature Geoscience 4:242-246. https://doi.org/10.1038/s41561-019-0326-6

Watanabe S, Tsuda Y, Yoshikawa M et al (2017) Hayabusa2 mission overview. Space Science Reviews 208:3-16. https://doi.org/10.1007/s11214-017-0377-1

Watanabe S, Hirabayashi M, Hirata N et al (2019) Hayabusa2 arrives at the carbonaceous asteroid 162173 Ryugu—A spinning top–shaped rubble pile. Science 364:268-272. https://doi.org/10.1126/science.aav8032

Wibben DR, Levine A, Russell JR et al (2024) OSIRIS-REx Earth Return & Entry: Targeting Strategy and Maneuver Performance. In 46th Annual AAS Guidance, Navigation and Control (GN&C) Conference.

Williams B, Antreasian P, Carranza E et al (2018) OSIRIS-REx flight dynamics and navigation design. Space Science Reviews 214:1-43. https://doi.org/10.1007/s11214-018-0501-x

Yabuta H, Cody GD, Engrand C et al (2023) Macromolecular organic matter in samples of the asteroid (162173) Ryugu. Science 379:eabn9057. https://doi.org/10.1126/science.abn9057

Yada T, Fujimura A, Abe M et al (2014) Hayabusa-returned sample curation in the Planetary Material Sample Curation Facility of JAXA. Meteoritics & Planetary Science 49:135-153. https://doi.org/10.1111/maps.12027

Yada T, Abe M, Okada T et al (2022) Preliminary analysis of the Hayabusa2 samples returned from C-type asteroid Ryugu. Nature Astronomy 6:214-220. https://www.nature.com/articles/s41550-021-01550-6

Yang B and Jewitt D (2010) Identification of magnetite in B-type asteroids. The Astronomical Journal 140:692-698. https://doi.org/10.1088/0004-6256/140/3/692

Yano H, Kubota T, Miyamoto H et al (2006) Touchdown of the Hayabusa spacecraft at the Muses Sea on Itokawa. Science 312:1350-1353. https://doi.org/10.1126/science.1126164

Yokoyama T, Nagashima K, Nakai I et al (2022) Samples returned from the asteroid Ryugu are similar to Ivuna-type carbonaceous meteorites. Science 379:eabn7850. https://doi.org/10.1126/science.abn7850

Yoshikawa M, Kawaguchi J, Fujiwara A et al (2021) The hayabusa mission. In Sample return missions 123-146. https://doi.org/10.1016/B978-0-12-818330-4.00006-9

Yurimoto H, Abe KI, Abe M et al (2011) Oxygen isotopic compositions of asteroidal

materials returned from Itokawa by the Hayabusa mission. Science 333:1116-1119. https://doi.org/10.1126/science.1207776

Zhang P, Zhang G, Yan X et al (2024) (469219) Kamoʻoalewa, A Space Weathering Matured Small NEA: Target of the Tianwen-2 Sample-Return Mission. Under Review, https://doi.org/10.21203/rs.3.rs-4281601/v1

Zeichner SS, Aponte JC, Bhattacharjee S et al (2023) Polycyclic aromatic hydrocarbons in samples of Ryugu formed in the interstellar medium. Science 382:1411-1416. https://doi.org/10.1126/science.adg6304

Zolensky M, Martinez J, Sitzman S et al (2022) Measuring the shock stage of Itokawa and asteroid regolith grains by electron backscattered diffraction, optical petrography, and synchrotron X-ray diffraction. Meteoritics & Planetary Science 57:1060-1078. https://doi.org/10.1111/maps.13808

Zolensky ME, Zega TJ, Yano H et al (2006) Mineralogy and petrology of comet 81P/Wild 2 nucleus samples. Science 314:1735-1739. https://doi.org/10.1126/science.1135842

https://ssd.jpl.nasa.gov/tools/sbdb_lookup.html#/?sstr=81P&view=OPDCA

https://blogs.nasa.gov/osiris-rex/2023/10/20/nasas-osiris-rex-achieves-sample-mass-milestone/

https://blogs.nasa.gov/osiris-rex/2024/02/15/nasa-announces-osiris-rex-bulk-sample-mass/